Magnetic Reconnection in Solar and Astrophysical Plasmas

K. Shibata
Kwasan Observatory, Kyoto University, Yamashina,
Kyoto 607-8471, Japan

ABSTRACT

Recent observations of magnetic reconnection in solar flares and related phenomena are reviewed with emphasis on the unified view emerging from the new observations. Magnetic reconnection in astrophysical plasmas is also discussed briefly.

1 INTRODUCTION

Recent progress from space solar observations such as Yohkoh (1991-2001), SOHO (1995-) and TRACE (1998-) has advanced solar physics significantly. With these space missions, it has been revealed that the solar corona is much more dynamic than had been thought, the quiet Sun is never quiet, the solar atmosphere is full of dynamic phenomena such as nanoflares, jets, waves, and shocks. Among the most important findings with these new observations is, perhaps, the notion that magnetic reconnection is ubiquitous in the solar atmosphere. A lot of direct and indirect evidence of magnetic reconnection has been found in solar flares and flare-like phenomena, and we can now say that the magnetic reconnection mechanism of solar flares is established, at least, phenomenologically, although there are a number of quantitative problems or puzzles remaining both observationally and theoretically as outlined in this article. The long-standing puzzle of the solar coronal heating mechanism is not yet solved, but these new observations suggest the possibility that even the quiet corona may be heated by small scale reconnection events such as microflares, nanoflares, or picoflares (e.g., [133], [10]).

Virtually all active phenomena occurring in the solar atmosphere seem to be related to magnetic reconnection, directly or indirectly. This is probably a consequence of the universal properties of magnetized plasmas: the solar corona is a low $\beta(= p_{gas}/p_{mag} \ll 1)$ plasma, where magnetic force and magnetic energy dominate other types of force and energy, so that magnetic reconnection has a great influence on heating and dynamics once it happens. There is evidence that even dynamic phenomena in the chromosphere (average $\beta \sim 1$) and photosphere (average $\beta \sim 10^4$) may be related to reconnection. This is also a result of the properties of magnetized plasma (e.g., [186]): Magnetic fields tend to be concentrated in thin filaments in high β plasmas, so that the magnetic energy density in these filaments is much larger than the average value. Hence, once reconnection occurs in these filaments, the influence of reconnection is not small.

On the other hand, recent astrophysical observations have revealed unprecedented activity in various astrophysical objects: the universe is full of jets, flares, and bursts, such as jets and flares in active galactic nuclei (quasars and radio galaxies), X-ray binaries, protostars, gamma-ray bursts, and so on. These are much more energetic than solar flares, but the basic observed properties of these explosive phenomena appear to be similar to those of solar flares. Though the evidence is still indirect, both theory and observations suggest a similarity between solar flares and astrophysical flares. It is argued that even tenuous hot plasmas in the interstellar medium, galactic halos, and intergalactic plasmas in clusters of galaxies may be heated by magnetic reconnection (e.g., [189], [103]).

In this article, we review recent progress made in studying observations of magnetic reconnection in solar flares and related phe-

nomena in the solar atmosphere, with emphasis on a unified view and unified model of solar flares and flare-like phenomena based on reconnection physics. The recent observations of astrophysical flares are also briefly mentioned.

General reviews related to solar flares and the corona are found in Aschwanden et al. [2], Hudson and Ryan [62], Hudson and Cliver [64], Kosugi and Shibata [80], Lang [92], Parker [135], Priest [139], Priest and Forbes [140][141], Sakai and de Jager [145], Shibata [160], and Tajima and Shibata [186].

2 BASIC PROPERTIES OF SOLAR CORONAL PLASMAS

Before going into details of observations, it would be instructive to give some basic information on the plasma properties of the solar corona.

The typical temperature (T) and electron density (n) of the solar coronal plasma are $1-2\times10^6$ K and 10^8 cm^{-3} (in quiet regions) -10^9 cm^{-3} (in active regions). Magnetic field strengths (B) in the corona range from a few G (in quiet regions) to about 100 G (in active regions). From these numbers, the micro-plasma scales such as Debye length (λ_D), ion Larmor radius (r_{Li}), electron inertial length (λ_e), and electron mean free path (λ_{mfp}) are found to be

$$\lambda_D = \Big(\frac{kT}{4\pi ne^2}\Big)^{1/2} \simeq 2\Big(\frac{T}{10^6\ \mathrm{K}}\Big)^{1/2}\Big(\frac{n}{10^9\ \mathrm{cm}^{-3}}\Big)^{1/2}\ \ \mathrm{cm}, \tag{1}$$

$$r_{Li} = \frac{c}{eB}(m_i kT)^{1/2} \simeq 10^2\Big(\frac{T}{10^6\ \mathrm{K}}\Big)^{1/2}\Big(\frac{B}{10\ \mathrm{G}}\Big)^{-1}\ \ \mathrm{cm}, \tag{2}$$

$$\lambda_e = \frac{c}{\omega_{pe}} \simeq 30\Big(\frac{n}{10^9\ \mathrm{cm}^{-3}}\Big)^{-1/2}\ \ \mathrm{cm}, \tag{3}$$

$$\lambda_{mfp} = v_{th,e}t_{coll} = \frac{m_e^2 v_{th,e}^4}{ne^4\ln\Lambda}$$
$$\simeq 10^7\Big(\frac{n}{10^9\ \mathrm{cm}^{-3}}\Big)^{-1}\Big(\frac{T}{10^6\ \mathrm{K}}\Big)^{2}\ \ \mathrm{cm}, \tag{4}$$

where ω_{pe} is the electron plasma frequency, $v_{th,e} = (kT/m_e)^{1/2}$ is the electron thermal speed, t_{coll} is the electron-ion collision time, and Λ is the coulomb logarithm with $\log\Lambda \simeq 10-100$.

On the other hand, the typical size of solar flares (L_{flare}) is

$$L_{flare} \simeq 10^9 - 10^{10}\ \ \mathrm{cm},$$

which is much larger than the micro-plasma scales. For pre-flare coronal plasmas, the flare size is larger than the electron mean free path, but for flare plasmas (with temperature $\sim 10^7$ K), the mean free path becomes comparable to the flare size. The electron-ion collision time is

$$t_{coll} \simeq 0.01\Big(\frac{n}{10^9\ \mathrm{cm}^{-3}}\Big)^{-1}\Big(\frac{T}{10^6\ \mathrm{K}}\Big)^{3/2}\ \ \mathrm{s} \tag{5}$$

and is about 0.01 s and 0.3 s for the pre-flare corona and flare plasmas, both of which are shorter than the typical flare time scale

$$t_{flare} \simeq 10 - 1000\ \mathrm{s}.$$

Hence, the collisional plasma (fluid) approximation seems to hold as far as macroscopic scales are concerned. However, because of the high magnetic Reynolds number

$$R_m = \frac{LV_A}{\eta} = \frac{t_{diff}}{t_A} \simeq$$

$$\simeq 10^{13}\Big(\frac{L}{10^9\ \mathrm{cm}}\Big)\Big(\frac{T}{10^6\ \mathrm{K}}\Big)^{3/2}\Big(\frac{B}{10\ \mathrm{G}}\Big)\Big(\frac{n}{10^9\ \mathrm{cm}^{-3}}\Big)^{-1/2} \tag{6}$$

in the solar corona, small scale current sheets, the thickness of which are much less than the mean free path, are easily formed in the reconnection region. Here,

$$\eta \simeq 10^4\Big(\frac{T}{10^6\ \mathrm{K}}\Big)^{-3/2}\ \ \mathrm{cm}^2\mathrm{s}^{-1} \tag{7}$$

is the magnetic diffusivity for Spitzer resistivity. Therefore, eventually we need knowledge of collisionless plasmas in and around the current sheets, and we also need to understand how the coupling occurs between macro-scales (flare size $\sim 10^9$ cm) and micro-scales (ion Larmor radius $\sim 10^2$ cm). Such an enormous gap between macro and micro scales (ratio of both scales $\sim 10^7$) is very different from the situation of plasmas in the laboratory and the magnetospheric current sheet where both scales are not so different, and are within a factor of 100 [191].

The situation in astrophysical plasmas is similar to the solar case or even more extreme: on stellar scales the magnetic Reynolds number is comparable to the solar value ($\sim 10^{13}$) or larger, and on galactic scales it is more than 10^{20}. The ratios of macro-scale to micro-scale are also much larger than unity, e.g., $> 10^9$ in the interstellar medium with $B = 10^{-6}$ G, $n_e = 1$ cm^{-3}, $T = 10^4 - 10^6$ K, and typical length scale $\sim 10^{18}$ cm.

Consequently, in solar and astrophysical plasmas, the magnetohydrodynamic (MHD) approximation can be used for most of the macro-scale dynamics, and the micro-scale plasma processes such as collisionless reconnection or anomalous resistivity become important only in a scale much smaller than the scale of interest or observations. The physics connecting macro-scales and micro-scales is a key to understanding magnetic reconnection occurrence in solar and astrophysical plasmas.

It should be remembered, however, that not only solar flares but also astrophysical jets and flares show strong nonthermal electromagnetic radiation, i.e., evidence of nonthermal particle acceleration. In order to understand the nonthermal particle acceleration mechanism, we have to understand the physics of collisionless plasmas. The particle acceleration mechanism is a difficult, challenging subject, and is beyond the scope of this paper. As for the particle acceleration in solar flares, the interested reader is referred to Miller et al. [120] and Aschwanden [4].

Finally, we discuss the macroscopic properties of the coronal plasma, such as the cooling properties. Since the coronal plasmas are hot and tenuous, heat conduction is very important and plasmas can be treated as optically thin. Hence the conduction and radiation cooling times in the corona are

$$t_{cond} \simeq \frac{3nkTL^2}{\kappa_0 T^{5/2}} \simeq 4\times 10^2\ \mathrm{sec}\ \Big(\frac{T}{10^6\ \mathrm{K}}\Big)^{-5/2}\Big(\frac{n}{10^9\ \mathrm{cm}^{-3}}\Big)\Big(\frac{L}{10^9\ \mathrm{cm}}\Big)^2, \tag{8}$$

$$t_{rad} \simeq \frac{3kT}{nQ(T)} \simeq 5 \times 10^3 \text{ sec } \Big(\frac{T}{10^6 \text{ K}}\Big)^{3/2} \Big(\frac{n}{10^9 \text{ cm}}\Big)^{-1}. \quad (9)$$

Here, $\kappa_0 \simeq 10^{-6}$ is the Spitzer's thermal conductivity parallel to the magnetic field, and

$$Q(T) \sim 10^{-22} \Big(\frac{T}{10^6 \text{ K}}\Big)^{-1/2} \text{ cgs} \quad \text{for } T < 10^7 \text{ K} \quad (10)$$

$$Q(T) \sim 3 \times 10^{-23} \Big(\frac{T}{10^7 \text{ K}}\Big)^{1/2} \text{ cgs} \quad \text{for } T > 10^7 \text{ K} \quad (11)$$

is the radiative loss function for optically thin plasma [144]. In the flare plasma, the temperature ($\sim 10^7$ K) is higher than that of the corona ($\sim 10^6$ K), and so the heat conduction is even more important. On the other hand, in the chromosphere, the temperature is low ($< 10^4$ K) and the density is large ($> 10^{11}$ cm^{-3}), so that heat conduction is not important and plasmas cannot be treated as optically thin. Hence, the radiation must be treated with the non-LTE radiative transfer equation.

3 FLARES AND PLASMOIDS

3.1 LDE FLARES

Solar observers have long thought that there are two types of flares, e.g., *long duration event (LDE) flares* and *impulsive flares*. LDE flares typically last more than 1 hour, while impulsive flares are short lived, less than 1 hour. The latter is characterized by impulsive hard X-ray emission whereas the former shows a softer X-ray spectrum.

The Yohkoh soft X-ray telescope (SXT; [194]) has revealed that many LDE flares show *cusp-shaped loop* structures [195], [197], [41] (Fig. 1), which are quite similar to the magnetic field cofiguration predicted by the classical magnetic reconnection model (Carmichael [24]- Sturrock [179]- Hirayama [55] -Kopp-Pneuman [78] model, called *CSHKP model*). [1] Although there were a few observations of cusp-shaped-like loops or arcades in the pre-Yohkoh era (e.g., [112], [48]), Yohkoh revealed a number of additional pieces of evidence of magnetic reconnection in LDE flares ([195] [197]):

[1] Here, the "CSHKP-type magnetic reconnection mechanism" simply means the *reconnection occurring in a helmet-streamer (or inverted Y type) field configuration* in which a vertical current sheet is situated above a closed loop. We should keep in mind that there was no agreement on the formation process of this geometry in Carmichael [24], Sturrock [179], Hirayama [55], and Kopp and Pneuman [78]. For example, Hirayama [55] considered that an MHD instability (causing filament eruption) is the key to forming this geometry, while Kopp and Pneuman [78] thought that the solar wind opened the closed field to form a current sheet. The only common point in these *classical models* is a helmet-streamer (or inverted Y type cusp-shaped) field configuration. I take this standpoint in this review for a definition of the "CSHKP" model. This model has been extended by many authors (e.g., some of such extended models are Cargill and Priest [22], Cliver [29], Forbes and Priest [38], Martens and Kuin [105], Moore and Roumeliotis [121]). As a historical remark, the term "CSHKP model" was first introduced by Sturrock [180] and Svestka and Cliver [184], and has often been used in the solar physics community.

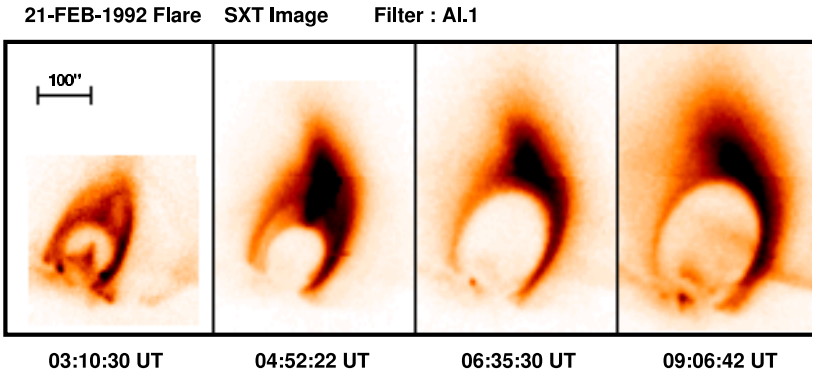

Figure 1: LDE flare on 21 Feb. 1992 observed with Yohkoh/SXT [195]. The images are negative. 100" corresponds to $\sim 7 \times 10^4$ km.

(1) The soft X-ray flare loops show not only a clear *cusp-shape* but also *apparent rise and expansion motion*, i.e., the heights of the loops and the separation of the two footpoints of the loops increase with time. The velocity of the rise motion of the loops, V_{loop}, is about 30 km/s in the early phase, and gradually decreases with time. The separation velocity of the loop footpoints, V_{foot}, is a bit smaller, ~ 10 km/s in the early phase, but shows a similar evolution. (This is an extension (i.e., X-ray version) of a well known feature of Hα post-flare loops and two-ribbon flares (e.g., [183], [7]).) These apparent velocities are interpreted to be a result of the accumulation of succesively reconnected field lines, and both velocities give us information on the reconnection inflow speed (V_{inflow}) through the magnetic flux conservation,

$$V_{inflow} B_{inflow} = V_{loop} B_{loop} = V_{foot} B_{foot}, \tag{12}$$

where $B_{inflow}, B_{loop}, B_{foot}$ are magnetic field strengths in the (coronal) inflow, loop top, and loop foot points, respectively.

(2) The *temperature* is systematically higher in the outer loops. The temperature is about $\sim 10^7$ K at the outer edge of the cusp loop, and decreases to 7×10^6 K at the loop top in the decay phase of the flare. The electron density is about a few $\times 10^{10}$ cm^{-3}. This temperature distribution is consistent with that predicted by the reconnection model since in this model the plasma is suddenly heated by reconnection near the outer edge of the cusp loops and then cooled gradually by heat conduction and radiative cooling, so that the inner loops tend to show a lower temperature (see Fig. 11 on the theoretical temperature distribution of reconnection-heated plasma [219], [220], [222]).

(3) The energy release rate and other physical quantities are consistent with predictions by the magnetic reconnection model (see the discussion in section 3.6).

The above evidence is found in almost all LDE flares. (Typical values above are for the 21 Feb. 1992 flare [195].) Furthermore, the following evidence of reconnection has been found in some events:

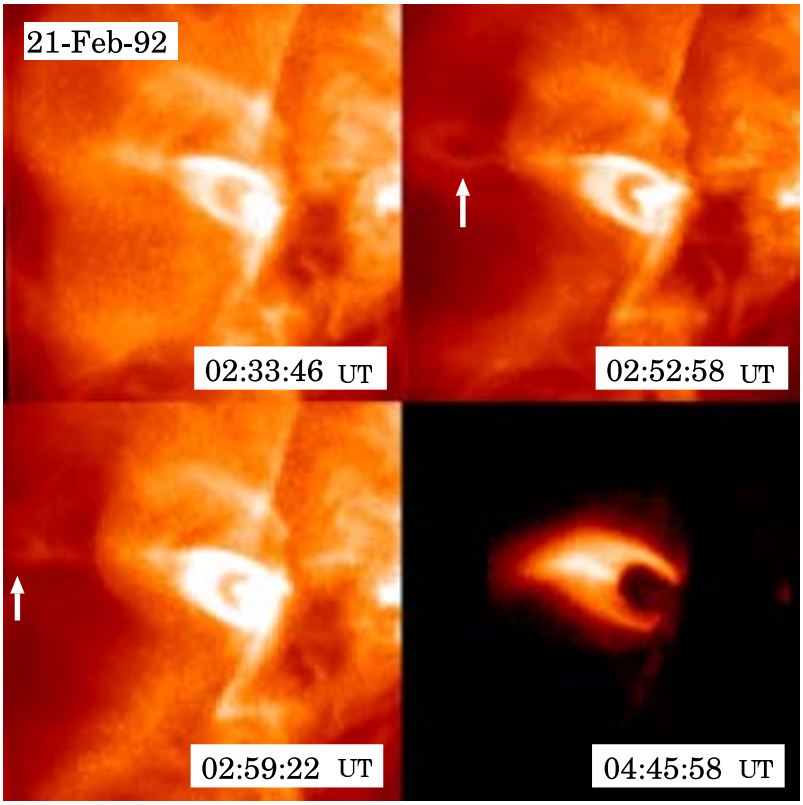

Figure 2: X-ray plamoid ejection from cusp-shaped LDE flare on 21 Feb. 1992 observed with Yohkoh/SXT ([61], [129]).

(4) X-ray *plasmoid ejections* are often seen in the rise phase of LDE flares (e.g., [61]; see Fig. 2). The velocity of ejection is of the order of a few 100 km/s. This is an X-ray version of Hα filament eruptions.

(5) The cusp gradually *shrinks* with time (Forbes and Acton 1996) as expected from reconnection theory, though the velocity is very small ($\sim$ a few km/s).

(6) *Downflows* with a speed of a few 100 km/s are found above the post flare loops in Yohkoh/SXT images ([116], [117], [115]; see Fig. 3), which is likely to be reconnection outflow as illustrated in Figure 3b.

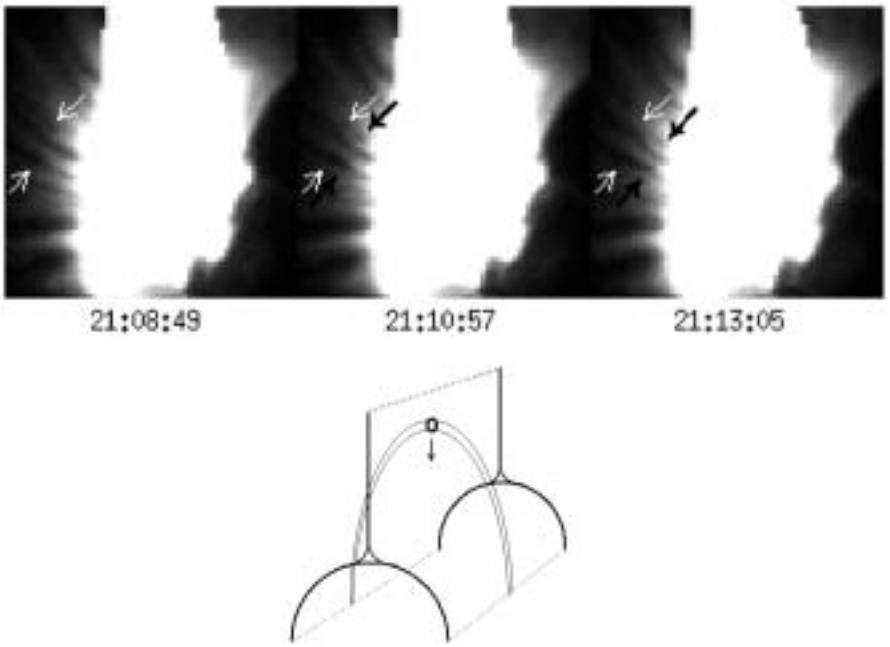

Figure 3: (a) Downflow above a flare arcade loop system in an LDE flare of 20 Jan 1998 observed with Yohkoh/SXT [116]. The black arrow indicates the apex of an X-ray emitting loop like feature, observed to shrink into the top of the arcade; the white arrow is at a fixed position, for comparison. The field of view is 2.2 $\times 10^5$ km square. (b) A schematic view of reconnection-induced downflow [117].

(7) The *reconnection inflow* (with $\sim$ 5 km/s) has been found in SOHO/EIT images of an LDE flare [223].

From these observations and analyses, it was established that LDE flares are produced by the CSHKP-type magnetic reconnection mechanism.

3.2 GIANT ARCADES

Cusp-shaped loops or arcades which show similar evolutional features to those of LDE flares have also been found on a much larger spatial scale [196], [54], [49],[113], [114], [75], [192], [69]. These large scale arcade formations, or simply *giant arcades*, usually occur in association with the disappearance of a dark filament and/or CMEs. Tsuneta et al. [196] described an event associated with the disappearance of a polar crown filament on Nov. 12, 1991. This event gradually increased its size over more than 20 hours to a size of 0.5 - 1.5 solar radius at maximum. Similar events occurred on Apr. 14, 1994 (Fig. 4), which were luckily reported by a KSC tohban ("duty operator" in Japanese) [2] to the world by Email, and the NOAA/SEL people then predicted the subsequent large geomagnetic storm successfully [114].

[2] See http://www.solar.isas.ac.jp/index.html for science nugget of August 2, 2002 for the word "tohban".

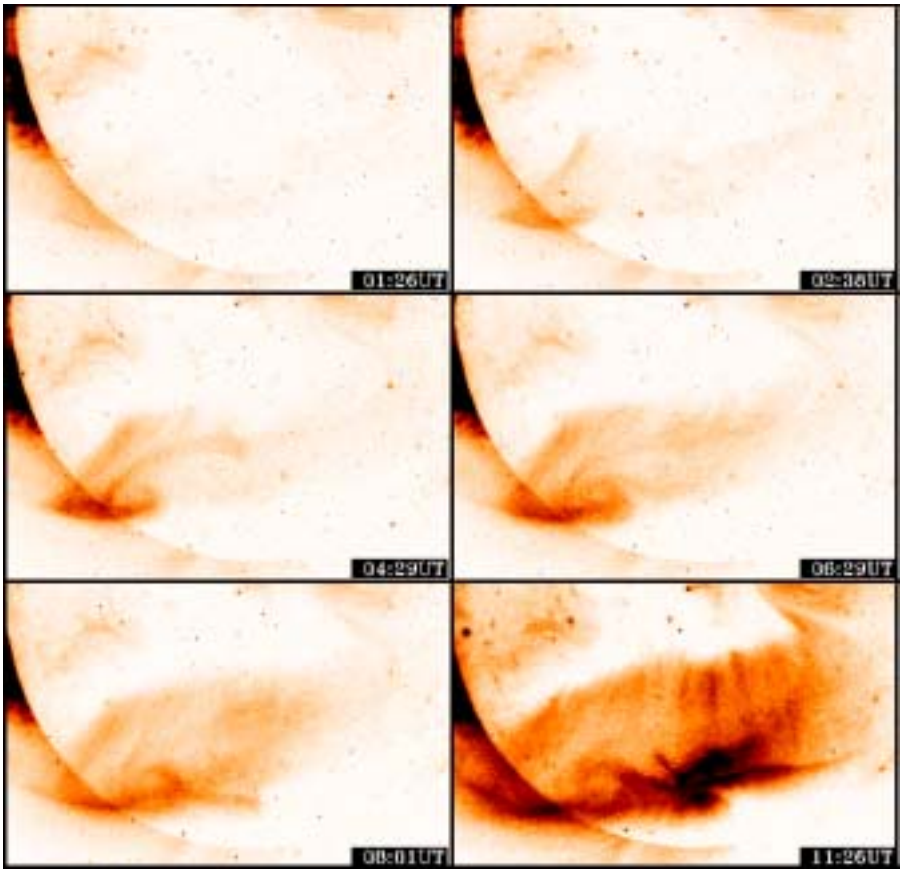

Figure 4: Giant arcade on 14 Apr. 1994 observed with Yohkoh/SXT [114].

A large helmet streamer appearing after a filament eruption and CME is possibly a side view of this kind of large scale arcade formation. A beautiful example of such a large helmet streamer formation occurred on Jan. 24, 1992 (Fig. 5), and was reported by Hiei et al. [54]. It is interesting to note that the temperature is higher at the outer edge of the cusp-shaped loops, which is similar to the case of LDE flares. Note also that the X-ray intensity of these events is usually very low so that often these cannot be noticed from GOES X-ray light curves. For this reason, these events were not considered to be flares [45]. However, Yohkoh/SXT has revealed that these giant arcades are very similar to LDE flares from various points of view (morphology, evolution such as the apparent rise motion of arcade-loops, emission measure and temperature distribution pattern, etc.). The only difference may be the size and magnetic field strength, which can also explain other differences, such as the time scale, total released energy, emission measure, etc., using scaling laws based on magnetic reconnection theory [214], [173]. Consequently, we can now say that these events are one class of flares.

Figure 5: Giant cusp-shaped loop (helmet streamer type feature) on 24 Jan. 1992 observed with Yohkoh/SXT [54]. Times are 24 Jan. 1992, 08:05UT, 14:33UT, 23:53UT, 25 Jan. 1992, 08:15UT, from the upper left to the lower right. The arrow shows the Y-shaped ejection feature, which may be a signature of slow and fast shocks just below the plasmoid (CME) [173].

There is now increasing evidence of reconnection in CMEs. Webb and Cliver [213] reported various pieces of evidence of magnetic disconnection in CMEs using pre-SOHO data. Recent SOHO/LASCO data show more evidence of magnetic disconnection and also flux rope (helical) structure in CMEs [174], [210], [33].

3.3 IMPULSIVE FLARES

Although LDE flares and giant arcades show clear cusp-shaped loop structures suggesting magnetic reconnection, there is no such cusp-shaped structure in *impulsive flares*, the occurrence frequency of which is greater than LDE flares. The impulsive flares are bright in hard X-rays and show an impulsive phase, the duration of which is short ($<$ a few minutes), whereas the LDE flares are usually weak in hard X-rays and do not necessarily show an impulsive phase. The apparent shape of the impulsive flares in SXT images is a *simple loop*, as already known from Skylab observations. Hence it was first thought that these impulsive flares might be created by a different mechanism from that of LDE flares, and even mechanisms other than reconnection have been proposed (e.g., Alfven and Carlqvist [6], Uchida and Shibata [202]).

It was Masuda [106] who changed this situation dramatically. He carefully coaligned the SXT and HXT (hard X-ray telescope; [79]) images of some impulsive compact loop flares observed at the limb, and showed that there is an impulsive HXR source *above* the SXR

loop, in addition to the footpoint impulsive double HXR sources [106], [108] (Fig. 6). Since the impulsive HXR sources are produced by high energy electrons which are closely related to the main energy release mechansim, this means that *the main energy release occurred above (outside) the SXR loop*. This means also that the flare models invoking the energy release site inside the SXR loops (e.g., [6], [175], [202]) must now be discarded at least for these impulsive compact loop flares.

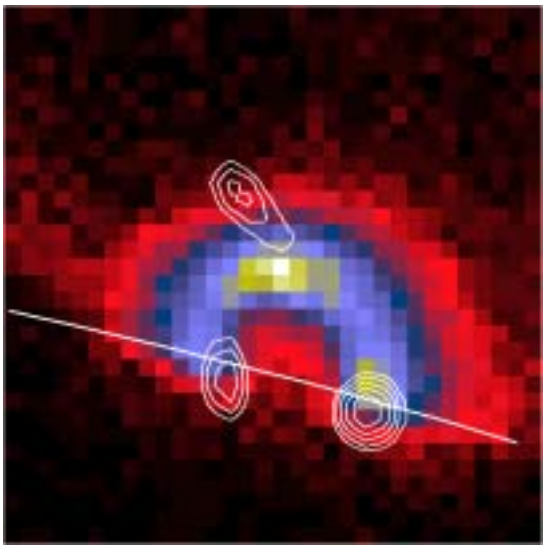

Figure 6: Impulsive flare on 13 Jan. 1992 observed with Yohkoh HXT and SXT, which shows a loop top hard X-ray source above the soft X-ray loop [107]. Contours of the hard X-ray (33 – 53 keV) intensity distribution are overlaid on the soft X-ray ($\sim$ 1 keV) image.

What is the energy release mechanism in these compact loop flares ? Masuda et al. [108] postulated that the basic magnetic field configuration is similar to that of LDE flares and that the high speed jet produced by reconnection collides with the top of the reconnected loop to produce a very hot region as well as high energy electrons. Later, Aschwanden et al. [1] found independent observational evidence that the acceleration site of high energy electrons is high above the SXR loops in Masuda type impulsive compact flares.

3.4 X-RAY PLASMOID EJECTIONS FROM IMPULSIVE FLARES

If the impulsive compact loop flares occur as a result of reconnection in a geometry similar to that of LDE flares, plasmoid ejections would be observed high above the loop top HXR source (Fig. 7; see also [56], [121]). Shibata et al. [157] searched for such plasmoid ejections using SXT images in 8 impulsive compact loop flares observed at the limb, which were selected by Masuda [107] in an unbiased manner. They indeed found that *all these flares were associated with X-ray plasma (or plasmoid) ejections*. The apparent velocities of these ejections are 50 – 400 km/s, and their height ranges are $4 - 10 \times 10^4$ km. Interestingly, flares with HXR sources well above the loop top show systematically higher velocities. The SXR intensity of the ejections is very low, typically $10^{-4} - 10^{-2}$ of the bright SXR loop. The

shapes of these plasma ejections are loop-like (e.g., 4 Oct 92 flare), blob-like (e.g., 5 Oct 92 flare [129], see Fig. 8; 2 Dec 91 flare [198]), or jet-like (e.g., 13 Jan 92 flare), and these are somewhat similar to the shapes of CMEs (e.g., [20]). In many cases, strong acceleration of the plasmoids occurs during the impulsive phase [128], [129] (Fig. 9; see also [72]), and the temporal relationship between the height of the ejections and the HXR intensity is very similar to that between the CME height and the SXR intensity of the associated flare [65], [224].

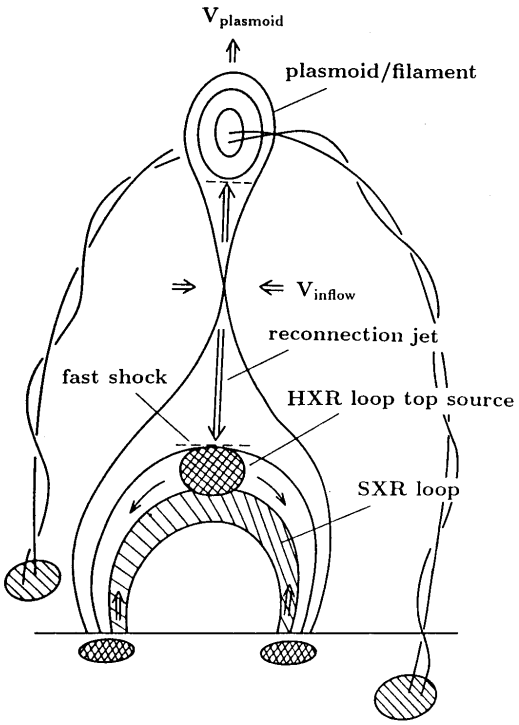

Figure 7: A unified model of flares: *plasmoid-induced-reconnection model* [157], [159], [161], [162],

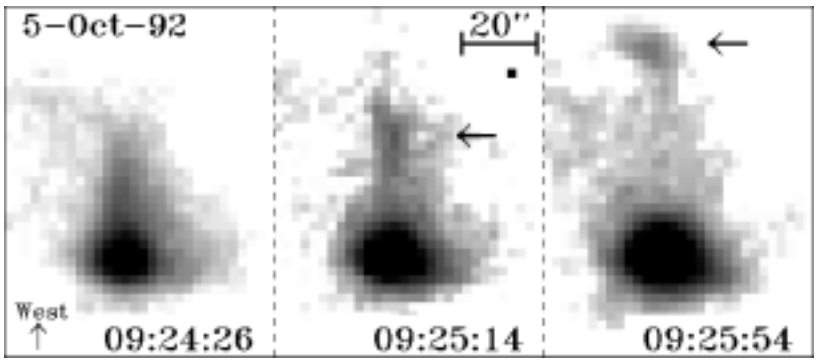

Figure 8: X-ray plasmoid ejections from an impulsive compact loop flare observed with Yohkoh SXT on 5 Oct. 1992 [129]. The velocity of the ejections is 200 – 450 km/s.

Ohyama and Shibata [128], [129] and Tsuneta [198] analyzed the

temperature distributions of plasmoids, flare loops, and the ambient structure, and revealed that the temperature of plasmoids is $\sim 6-13$ MK, and the overall temperature distribution is consistent with that predicted by the reconnection model. Ohyama and Shibata [128], [129] showed that the kinetic energy of plasmoids is much smaller than that of the total flare energy. This means that the kinetic energy of the plasmoid ejection cannot be the source of the flare energy. Instead, the plasmoid ejection could play a role in triggering the main energy release in the impulsive phase, since in some events observed from the preflare phase it was found that the plasmoid ejection started (at 10 km/s) well before the impulsive phase ([128]; Fig. 9).

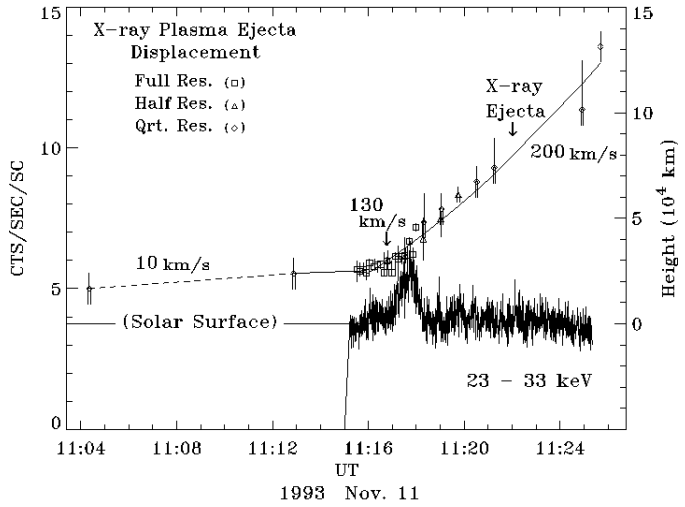

Figure 9: Temporal variations of the height of an X-ray plasmoid and the hard X-ray intensity in an impulsive flare on 11 Nov. 1993 observed by Yohkoh SXT and HXT (from [128]).

In an attempt to identify the direct signature of CMEs in soft X-rays, Nitta and Akiyama [126] searched for plasma ejections in Yohkoh/SXT images in a total of 17 limb flares, and compared the results with SOHO/LASCO data. They found that a general correlation exists between the X-ray ejection and the CME.

What is the universality of X-ray plasma ejections in flares ? Ohyama and Shibata [130] examined 57 limb flares (larger than GOES C-class) between October 1991 and August 1998, whose observing time cadence was good enough to study the timing relationship. They found X-ray plasma ejections in 100 % of X-class flares, and 74-82 % of M-class flares, whereas only 31-38 % of C-class flares had X-ray plasma ejections. Considering the difficulty in detecting X-ray plasma ejections in C-class flares, because of their small size and short lifetime, these results suggest that X-ray plasma ejections are a general phenomenon associated with solar flares.

3.5 OBSERVED RECONNECTION RATE

Yokoyama et al. [223] discovered clear evidence of reconnection inflow in an LDE flare as described above, and derived the reconnection rate,

$$M_A = V_{inflow}/V_A \simeq 0.001 - 0.03.$$

So far, this is the only "direct" observation of reconnection inflow, i.e., direct measurement of the reconnection rate.

Dere [32] examined the time scale τ and the spatial scale L of reconnection events in the solar corona and found L/τ to be $0.01 - 0.1V_A$ for these events. Tsuneta [197] derived the reconnection rate for an LDE flare by estimating the half-angle of slow shocks from SXT images, assuming Petschek type reconnection. Tsuneta et al. [199] and Ohyama and Shibata [128], [129] also used the SXT data and considered the energy release rate

$$\frac{dE_{th}}{dt} = 2\frac{B^2_{corona}}{4\pi}V_{inflow}A, \tag{13}$$

where $E_{th} = 3nkT$ is the thermal energy content of a flare loop, and A is the area of the reconnection region, both of which are observable. To obtain B_{corona} and V_{inflow}, they assumed pressure balance

$$p_{in} = p_{out} + B^2_{corona}/8\pi,$$

where p_{in} and p_{out} are the gas pressures inside and outside of the current sheet. If we assume these gas pressures are comparable to the gas pressure of flare loop observed with Yohkoh/SXT, we can estimate B_{corona}, and hence v_{inflow}, from the above equation. Isobe et al. [68], instead, used the magnetic flux conservation equation (eq. 12),

$$V_{inflow}B_{corona} = V_{foot}B_{foot},$$

where V_{foot} is the separation velocity of the two feet of a flare arcade loop, and B_{foot} is the photospheric magnetic field strength at the foot of the loop. Since both V_{foot} and B_{foot} are observables, we can determine the reconnection rate from these two equations without further assumptions. Isobe et al. [68] estimated the reconnection rate in this way, and found $M_A \simeq 0.001 - 0.01$ for the decay phase of an LDE flare. Talbe 1 summarizes observed reconnection rates.

Table I Observed Reconnection Rate (Isobe et al. [68])

Author	Reconnection Rate (V_{inflow}/V_A)	Event
Dere [32]	0.001-0.1	Many events
Tsuneta [197]	0.07	1992 Feb 21
Tsuneta et al. [199]	0.06	1992 Jan 13
Ohyama & Shibata [128]	0.0002-0.013	1993 Nov 11
Ohyama & Shibata [129]	0.02	1992 Oct 5
Yokoyama et al. [222]	0.001-0.03	1999 Mar 18
Isobe et al. [68]	0.001-0.01	1997 May 12

3.6 RECONNECTION MODEL

3.6.1 Energy Release Rate

The magnetic energy stored around the current sheet and the plasmoid is suddenly released through reconnection into kinetic and thermal/nonthermal energies after the plasmoid is ejected. The magnetic energy release rate at the current sheet (with a length of $L_{inflow} \simeq 2 \times 10^4$ km) is estimated to be

$$\frac{dW}{dt} = 2 \times L_{inflow}^2 B^2 V_{inflow}/4\pi$$
$$\sim 4 \times 10^{28} \Big(\frac{V_{inflow}}{100 \text{ km/s}}\Big)\Big(\frac{B}{100 \text{ G}}\Big)^2\Big(\frac{L_{inflow}}{2 \times 10^9 \text{ cm}}\Big)^2 \text{ erg/s}. \quad (14)$$

This is comparable to the energy release rate during the impulsive phase, $4-100 \times 10^{27}$ erg/s, estimated from the HXR data, assuming the lower cutoff energy as 20 keV [106]. In this model, the electric field at the X-point (and surrounding region) becomes

$$E \sim V_{inflow} B/c \simeq 10^3\Big(\frac{V_{inflow}}{100\text{km/s}}\Big)\Big(\frac{B}{100\text{G}}\Big) \text{ V/m}, \quad (15)$$

and is largest during the impulsive phase. Hence, it naturally explains the acceleration of higher energy electrons in the impulsive phase: observed nonthermal electron energies 10 keV $-$ 1MeV are explained if electrons can travel along this electric field for a path of $10 - 1000$ m, which is much shorter than the actual macro-scale size of flares. Such a situation may be possible if there is a magnetic field perpendicular to the plane at the neutral point (e.g., [98]).

3.6.2 Reconnection Jets and Fast Shocks

The magnetic reconnection theory predicts two oppositely directed high speed jets from the reconnection point at Alfven speed,

$$V_{jet} \sim V_A \simeq 2000\Big(\frac{B}{100\text{G}}\Big)\Big(\frac{n_e}{10^{10}\text{cm}^{-3}}\Big)^{-1/2} \text{ km/s}, \quad (16)$$

where B is the magnetic flux density and n_e is the electron density. The downward jet collides with the top of the SXR loop, producing MHD fast shock [205], [3] superhot plasmas and/or high energy electrons at the loop top, as observed in the HXR images. The temperature just behind the fast shock becomes

$$T_{loop-top} \sim m_i {V_{jet}}^2/(6k) \sim$$
$$2 \times 10^8 \Big(\frac{B}{100\text{G}}\Big)^2\Big(\frac{n_e}{10^{10}\text{cm}^{-3}}\Big)^{-1} \text{ K}, \quad (17)$$

where m_i is the hydrogen ion mass and k is the Boltzmann constant. This explains the observationally estimated temperature of the loop top HXR source when the source is thermal [107]. However, it should be noted that it is still not yet clarified whether the source is thermal or nonthermal. Tsuneta and Naito [200] presented a model for particle acceleration at the fast shock just below the reconnection jet to explain the loop top HXR source (assuming that the source is nonthermal) and nonthermal double foot point HXR sources.

[3] Aurass et al. [9] found an interesting signature of fast shocks just below reconnection jet in radio observations.

3.6.3 Slow Shock and an Effect of Heat Conduction

Petschek's reconnection model predicts the formation of a pair of slow shocks propagating from the reconnection point (diffusion region). In the adiabatic case, the temperature behind the slow shocks becomes

$$T_{slow,adiabatic} \sim \frac{B^2}{16\pi nk}$$
$$\simeq 2 \times 10^8 \text{ K } \Big(\frac{B}{100\text{G}}\Big)^2 \Big(\frac{n}{10^{10}\text{cm}^{-3}}\Big)^{-1}. \quad (18)$$

As discussed in section 1, however, heat conduction is very important in the flare plasmas, and its effect must be considered in the slow shock structure. For a typical flare plasma with $T = 10^7$ K, $n = 10^{10}$ cm^{-3}, $L \sim 10^9$ cm, the heat conduction time is $t_{cond} \sim 10$ sec, whereas the radiative cooling time is $t_{rad} \sim 10^4$ sec. On the other hand, the Alfven time is $t_A = L/V_A \sim 5$ sec. Hence t_{cond} is comparable to t_A. This means that the heat conduction length at the slow shock front is comparable to the system size, $L \sim 10^9$ cm. That is, in a typical flare, *adiabatic slow shocks dissociate into conduction fronts and isothermal slow shocks* [39]. Yokoyama and Shibata [219] numerically simulated reconnection coupled with heat conduction for the first time, and confirmed this property of the slow shock structure (Fig. 10).

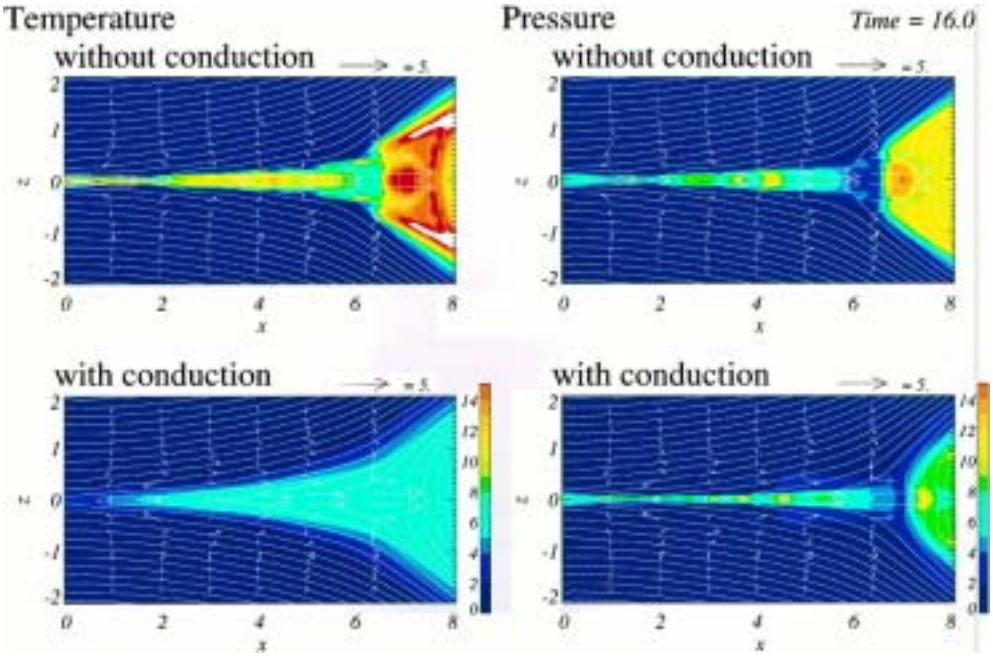

Figure 10: Numerical simulation of reconnection coupled with heat conduction [219].

Tsuneta [197] argued that the temperature distribution obtained from Yohkoh soft X-ray images of a typical LDE flare (Fig. 1) revealed evidence of slow shocks. As we discussed above, however, the outer edge of the cusp is not a slow shock but a conduction front. The (isothermal) slow shock has not yet been identified. To detect slow shocks will be one of the most important subjects in the future Solar B mission.

Yokoyama and Shibata [220] [222] extended their simulations to include chromospheric evaporation (e.g., [58]), and found the following temperature scaling law:

$$T_{max} \simeq \Big(\frac{B^2 V_A L}{\kappa_0 2\pi}\Big)^{2/7}$$

$$\simeq 3\times 10^7 \ \mathrm{K}\Big(\frac{B}{50\mathrm{G}}\Big)^{6/7}\Big(\frac{n_0}{10^9\mathrm{cm}^{-3}}\Big)^{-1/7}\Big(\frac{L}{10^9\mathrm{cm}}\Big)^{2/7}. \qquad (19)$$

Here, n_0 is the pre-flare plasma density. This relation is derived from the balance between the conduction cooling, $\kappa_0 T^{7/2}/(2L^2)$, and reconnection heating, $(B^2/4\pi)(V_A/L)$. This temperature ($\sim$ 30 MK) is a bit higher than the typical temperature of flare loops ($\sim$ 10 MK), and hence may well be applied to superhot components above soft X-ray loops (e.g., [95], [106], [124]). The temperature of the main flare loop observed in soft X-rays is about 1/3 cooler than the maximum temperature [220] [222] so that the "flare temperature" (i.e., the temperature with the largest emission measure) is approximately given by the following formula:

$$T_{flare} \simeq 10^7 \ \mathrm{K}\Big(\frac{B}{50\mathrm{G}}\Big)^{6/7}\Big(\frac{n_0}{10^9\mathrm{cm}^{-3}}\Big)^{-1/7}\Big(\frac{L}{10^9\mathrm{cm}}\Big)^{2/7}. \qquad (20)$$

3.6.4 Plasmoids-Induced-Reconnection and Fractal Reconnection

What is the role of plasmoid ejections in flares ? Are plasmoids simply a biproduct of reconnection ? Or are the plasmoid ejections a cause of reconnection ?

On the basis of Yohkoh observations, Shibata [159], [161], [162] proposed the *plasmoid-induced-reconnection model*, by extending the classical CSHKP model. In this model, the plasmoid ejection plays a key role in triggering fast reconnection in two different ways. [4]

1) *A plasmoid (flux rope) can store energy by inhibiting reconnection.* A large magnetic island (plasmoid or flux rope) inside the current sheet is a big obstacle for reconnection. Hence if an external force compresses the current sheet, magnetic energy can be stored around the current sheet. Only after the plasmoid is ejected out of the current sheet, will the anti-parallel field lines be able to touch and reconnect. If a larger plasmoid is ejected, a larger energy release occurs.

2) *A plasmoid ejection can induce a strong inflow into the reconnection site.* If a plasmoid is suddenly ejected out of the current sheet at the velocity $V_{plasmoid}$, an inflow must develop toward the X-point in order to compensate for the mass ejected by the plasmoid, as has been shown in many numerical simulations (e.g., [204], [40], [216], [222], [101], [190]). The inflow speed can be estimated from the mass conservation law (assuming incompressibility for simplicity);

$$V_{inflow} \sim V_{plasmoid} W_{plasmoid}/L_{inflow}, \qquad (21)$$

where $W_{plasmoid}$ is the typical width of the plasmoid, and $L_{inflow}(\geq W_{plasmoid})$ is the typical vertical length of the inflow region. In deriving equation (21), it is assumed that the mass flux into the reconnection region ($\sim L_{inflow} V_{inflow}$) is balanced by the mass flux

[4] In this model, on the basis of observations, we *assume* that the plasmoid is already created before the flare, and is suddenly accelerated by some mechanism. Magnetic reconnection might also play a role in the preflare phase as noted by Ohyama and Shibata [160]. See also related theoretical studies by Kusano et al. [91], Kitabata et al. [76], Magara et al. [101].

carried by the plasmoid motion ($\sim V_{plasmoid} W_{plasmoid}$). Since the reconnection rate is determined by the inflow speed, the ultimate origin of the fast reconnection in this model is the fast ejection of the plasmoid. If the plasmoid ejection (or outflow) is inhibited in some way, then fast reconnection ceases [203], [190], [94].

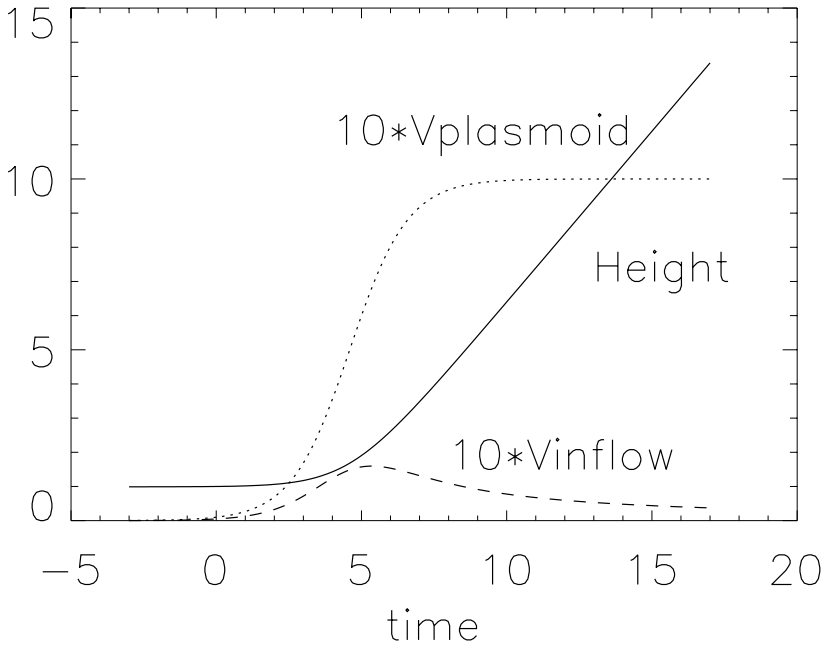

Figure 11: Temporal variations of the plasmoid velocity (V_p), its height, and inflow velocity (V_i) in an analytical model [164] for the case of $V_A/V_0 = 100$. Units of the velocity, height, and time are V_A, L_p, and L_p/V_A, respectively.

Shibata and Tanuma [164] presented a simple analytical model (Fig. 11), in which the plasmoid ejection and acceleration are closely coupled with the reconnection process. In this model, the coupling between the plasmoid acceleration and the reconnection leads to a *nonlinear instability* for all the dynamics that determine the macroscopic reconnection rate uniquely. This model naturally explains (1) the strong acceleration of plasmoids during the impulsive (rise) phase of flares (see Fig. 9), (2) the positive correlation between the plasmoid velocity and the apparent rise velocity of flare loops [157], [164], (3) the total energy release rate of flares and plasmoid ejections [160], and (4) the time scale of the impulsive (rise) phase for both impulsive flares ($\sim L_{inflow}/V_{plasmoid} \sim 10^4$ km/100 km/s $\sim$ 100 sec), and for LDE flares ($\sim 10^5$ km/100 km/s $\sim 10^3$ sec).

It is interesting to note that similar impulsive reconnection associated with plasmoid ejection (current sheet ejection) has also been observed in laboratory experiments [132].

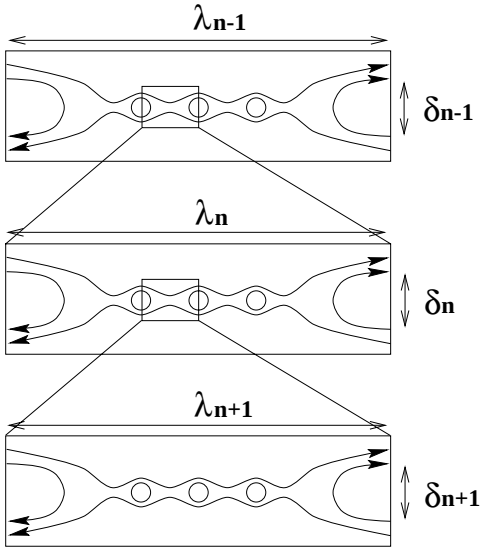

Figure 12: Schematic view of fractal reconnection [164].

Shibata and Tanuma [164] further showed that the current sheet tends to have a *fractal structure* via the following process path (Fig. 12): tearing ⇒ sheet thinning ⇒ Sweet-Parker sheet ⇒ secondary tearing ⇒ further sheet thinning ⇒ ... These processes occur repeatedly at smaller and smaller scales until a microscopic plasma scale (either the ion Larmor radius or the ion inertial length) is reached and anomalous resistivity or collisionless reconnection can occur. The current sheet eventually has a fractal structure with many plasmoids (magnetic islands) of different sizes (see Hoshino et al. [59] for similar processes in the magnetotail). When these plasmoids are ejected out of the current sheets, fast reconnection occurs at various different scales in a highly time dependent manner (Fig. 13). This kind of *fractal reconnection* naturally explains the 1/f-like time variability of the nonthermal radio and hard X-ray emissions observed during the impulsive phase of solar flares [14], [77], [4].

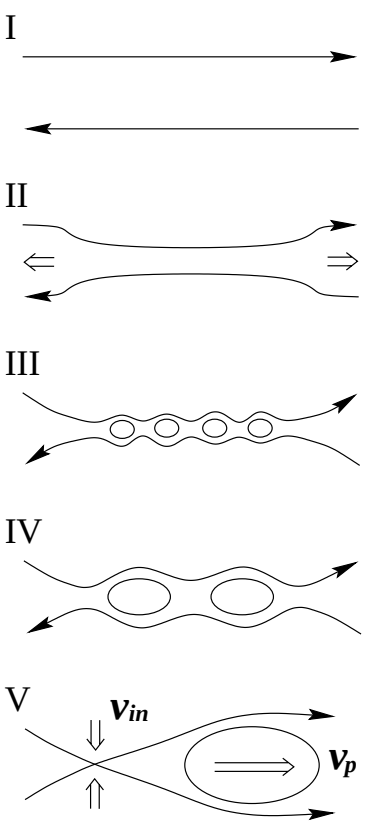

Figure 13: A scenario for fast reconnection [164]. I: The initial current sheet. II: The current sheet thinning in the nonlinear stage of the tearing instability or global resistive MHD instability. The current sheet thinning stops when the sheet evolves to the Sweet-Parker sheet. III: The secondary tearing in the Sweet-Parker sheet. The current sheet becomes fractal because of further secondary tearing as shown in Fig. 12. IV: The magnetic islands coalesce to form bigger magnetic islands. The coalescence itself proceeds in a fractal nature. In the phases III and IV, the microscopic plasma scale (ion Larmor radius or ion inertial length) is reached, so that fast reconnection becomes possible at small scales. V: The greatest energy release occurs when the largest plasmoid (magnetic island or flux rope) is ejected. The maximum inflow speed (V_{in} = reconnection rate) is determined by the velocity of the plasmoid (V_p). Hence this reconnection is named *plasmoid-induced-reconnection*.

3.6.5 Numerical Modeling

Here we briefly mention numerical modeling of flares and associated mass ejections (as a model of coronal mass ejections). There are several different kinds of numerical models so far: (1) sheared arcade model ([118], [16], [91], [27], [28], [60]), (2) converging arcade model [40], (3) emerging flux triggering model [26] (see Figs. 14 and 15), (4) converging flux or quadrupole model [57].

It is interesting to note that all these models show strong coupling between the plasmoid ejection and fast reconnection. Namely, if we artificially inhibit fast reconnection, there is no fast plasmoid ejection. On the other hand, if we inhibit plasmoid ejection, fast reconnection suddenly stops even if we drive reconnection strongly in the initial state. In the sheared arcade model, the arcade becomes unstable for resistive MHD instability similar to the tearing instability (see also [101]), but the ejection speed of the plasmoid is slow if the reconnection is slow. Only when both fast reconnection and plasmoid ejection occur, does fast ejection of the plasmoid (i.e., CMEs) become possible as a result of the strong coupling between reconnection and plasmoid ejection, as mentioned above.

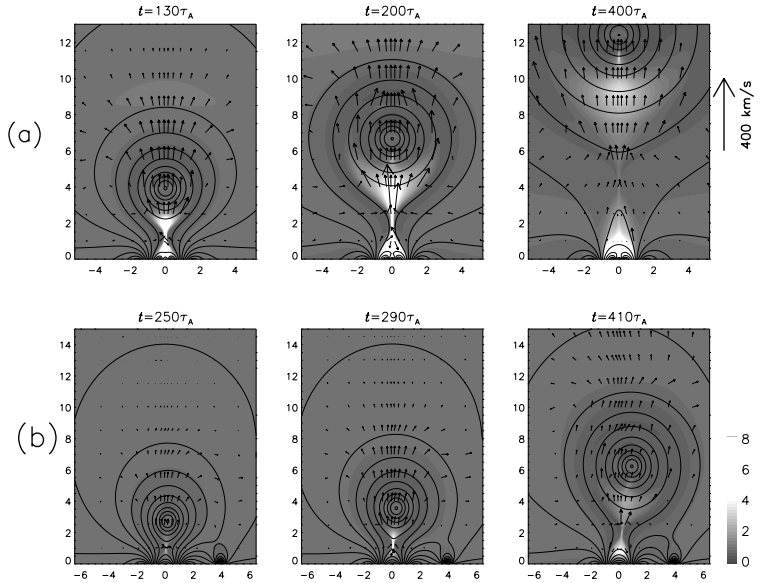

Figure 14: Numerical simulation of emerging flux triggering model of solar flares and CMEs [26]. (a) Case A: emerging flux appeared just below a filament. (b) Case B: emerging flux appeared at a distant place from the filament.

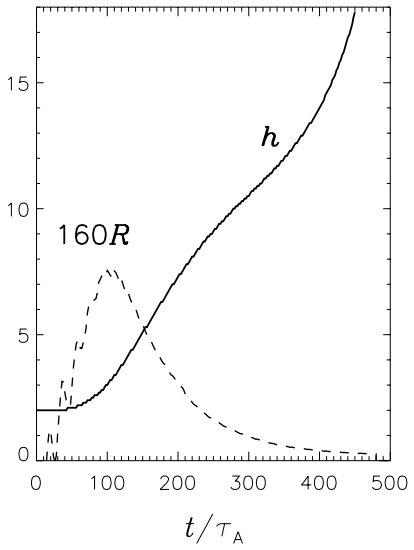

Figure 15: The time profiles of the reconnection rate (R) and the height of the flux rope (h) in case A in Fig. 14. The solid line is for h, and the dashed line is for R [26].

4 MICROFLARES AND JETS

4.1 TRANSIENT BRIGHTENINGS (MICROFLARES)

Shimizu et al. [166], [167] analyzed *active region transient brightenings (ARTBs)* in detail, and found that these correspond to the soft X-ray counter part of hard X-ray microflares [96], [30]. The total

thermal energy content of ARTBs is $10^{25} - 10^{29}$ erg, their lifetime ranges from 1 to 10 min, their length is $(0.5 - 4) \times 10^4$ km, and the temperature is about $6 - 8$ MK. According to a recent analysis by Shimizu et al. [169] on the comparison of Yohkoh SXT images of ARTBs with simultaneous visible light observations at LaPalma, some ARTBs occur in association with emergence of tiny magnetic bipoles, suggesting reconnection between emerging flux and the pre-existing field.

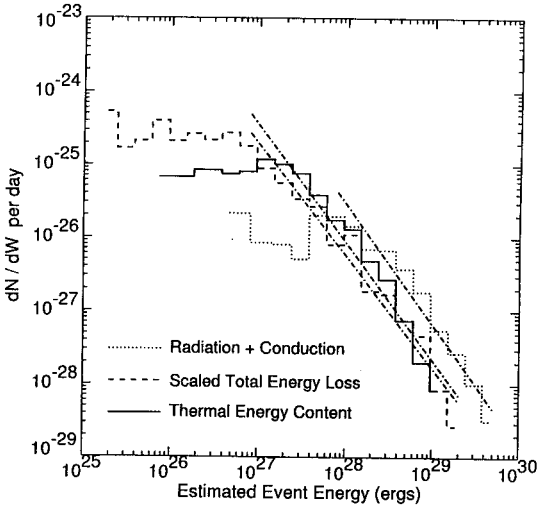

Figure 16: Frequency distribution of transient brightenings (microflares) as a function of the total energy estimated with three different methods (taken from Shimizu [168]. Each distribution can be represented by a single power law with the index 1.5 – 1.6 (dash-dotted lines).

The occurrence frequency of these ARTBs (SXR microflares) decreases with increasing total energy and shows a power-law distribution;

$$dN/dE \propto E^{-\alpha}, \tag{22}$$

where dN is the number of ARTBs per day in the energy range between $E + dE$ and E, and $\alpha \simeq 1.5 - 1.6$ ([168]; see Fig. 16). This is nearly the same as that of hard X-ray (HXR) microflares and larger flares. Since the index α is less than 2, the SXR microflares alone cannot explain coronal heating. [5] The universal power-law distribution seems to suggest a universal physical origin for both microflares and large scale flares [208].

From simultaneous observations by the VLA and Yohkoh, Gopalswamy et al. [44] found microwave counterparts of ARTBs. Kundu et al. [87] observed type III bursts in association with an XBP flare, which means that XBP flares are similar to normal flares and can accelerate nonthermal electrons.

Koutchmy et al. [81], [82] have found even less energetic transient brightenings in polar regions which they call *coronal flashes*. The absolute SXR intensity of flashes is about 10 DN/s at maximum, which is two orders of magnitude smaller than those of ARTBs, and fluctuates on a time scale of a few – 5 min. The total (released)

[5] Porter et al. [138], Krucker and Benz [85], Benz and Krucker [15], however, claimed that EUV microflares/nanoflares show a power law index larger than 2. See Aschwanden and Parnell [3] for more recent references related to this subject.

energy is probably comparable to 10^{24} erg, i.e., that of nanoflares. The polar coronal holes are found to be very active and full of these nanoflares, and tiny X-ray jets often occur from these nanoflares.

4.2 X-RAY JETS

X-ray jets are defined as transitory X-ray enhancements with apparent collimated motion [154], [155], [156], [158], [178], [170], [172]. Almost all jets are associated with microflares or subflares, and the length ranges from 1000 to 4×10^5 km. No one knows their true (Doppler shift) velocity; their apparent velocity is 10 – 1000 km/s. The temperature of X-ray jets is about 4 – 6 MK, which is comparable to those of the footpoint microflares. The electron density ranges from 3×10^8 to 5×10^9 cm^{-3} and the kinetic energy is estimated to be $10^{25} - 10^{29}$ erg. Figure 17 shows a typical example of an X-ray jet with a length $\sim 2 \times 10^5$ km and a velocity of more than 100 km/s.

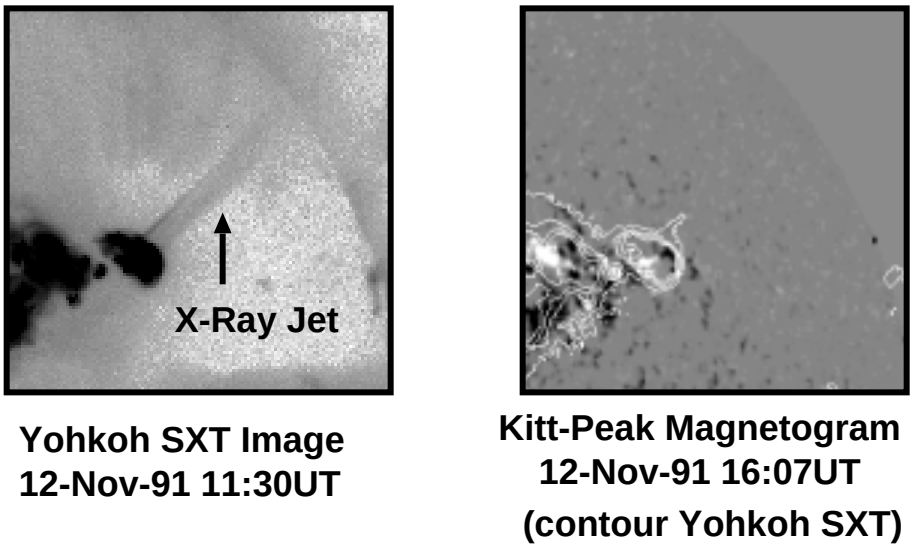

Figure 17: Left: An X-ray jet observed with Yohkoh SXT on 12 Nov. 1991 [154]. Right: NSO/Kitt Peak magnetogram for the same region with overlay contours of the soft X-ray intensity distribution. Note the mixed polarities at the footpoint of the jet.

There are several pieces of evidence of magnetic reconnection in X-ray jets.

(1) *Morphology*: Many jets show a constant or converging shape [170], implying a magnetic field configuration with a neutral point near the footpoint of the jet as shown in Figure 18. In some jets, a gap is seen between the footpoints of the jets and the brightest part of the footpoint flares. This is also explained by the reconnection model [170] since reconnection creates two hot reconnected field lines (a loop and a jet) with a gap between them. Shibata et al. [155] noted that there are two types of interaction between emerging flux and the overlying coronal field; one is the *anemone-jet* type, in which emerging flux appears in a coronal hole and a jet is ejected vertically, and the other is the *two-sided-loop* type, which occurs when the

emerging flux appears in a quiet (closed loop) region, producing two-sided loops (or jets). The morphology of these types is suggestive of reconnection between emerging flux and the overlying coronal field and the resultant formation of jets (or loop brightenings).

(2) *Magnetic field*: Shimojo, Harvey, and Shibata [171] showed that the magnetic field properties of the footpoints of jets are mainly mixed polarities or satellite spots. This gives direct evidence of the presence of neutral points (or current sheets) near the footpoints of jets.

(3) *Hα surges*: Often Hα surges are associated with X-ray jets (e.g., [154], [21]), though there are also negative cases [148]. From observations of Hα surges associated with X-ray jets, Canfield et al. [21] found several new pieces of evidence of reconnection.

(4) *Type III bursts*: Kundu et al. [88] found that some X-ray jets are associated with type III bursts (see also [8], [143]). This indicates that high energy electrons are accelerated in these small scale microflare/jet events, suggesting that the same physical process as that of larger flares (i.e., magnetic reconnection) might be occurring in these events.

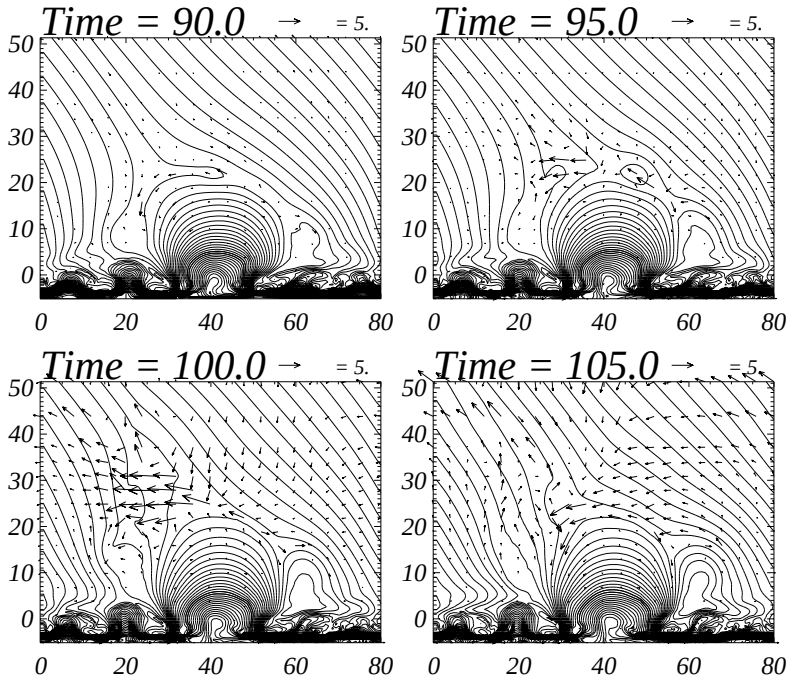

Figure 18: Emerging flux reconnection model of Yokoyama and Shibata [217], [218]. Note that plasmoids (magnetic islands) are repeatedly created in the current sheet.

4.3 EMERGING FLUX RECONNECTION MODEL

Yokoyama and Shibata [217], [218] developed a magnetic reconnection model of X-ray jets using 2.5D MHD numerical simulations (Figs. 18 and 19). In their model, magnetic reconnection occurs in the current sheet between emerging flux and the overlying coronal field as in the classical emerging flux model [53], [38], [153]. The basic driving force is magnetic buoyancy, though the reconnection rate

is not uniquely determined by the rise velocity of the emerging flux, but is affected by the local plasma conditions such as the resistivity and dynamics [204], [206], [149], [216]. Yokoyama and Shibata [217] [218] found several interesting features in their simulation results based on this emerging flux model.

(1) *Plasmoids*: The reconnection starts with the formation of magnetic islands (i.e., plasmoids). (In three dimensions, they are seen as helically twisted flux ropes.) These islands coalesce with each other due to a coalescence instability (e.g., [37], [185]) and finally are ejected out of the current sheet (Fig. 18). After the ejection of the biggest island, the largest energy release occurs.

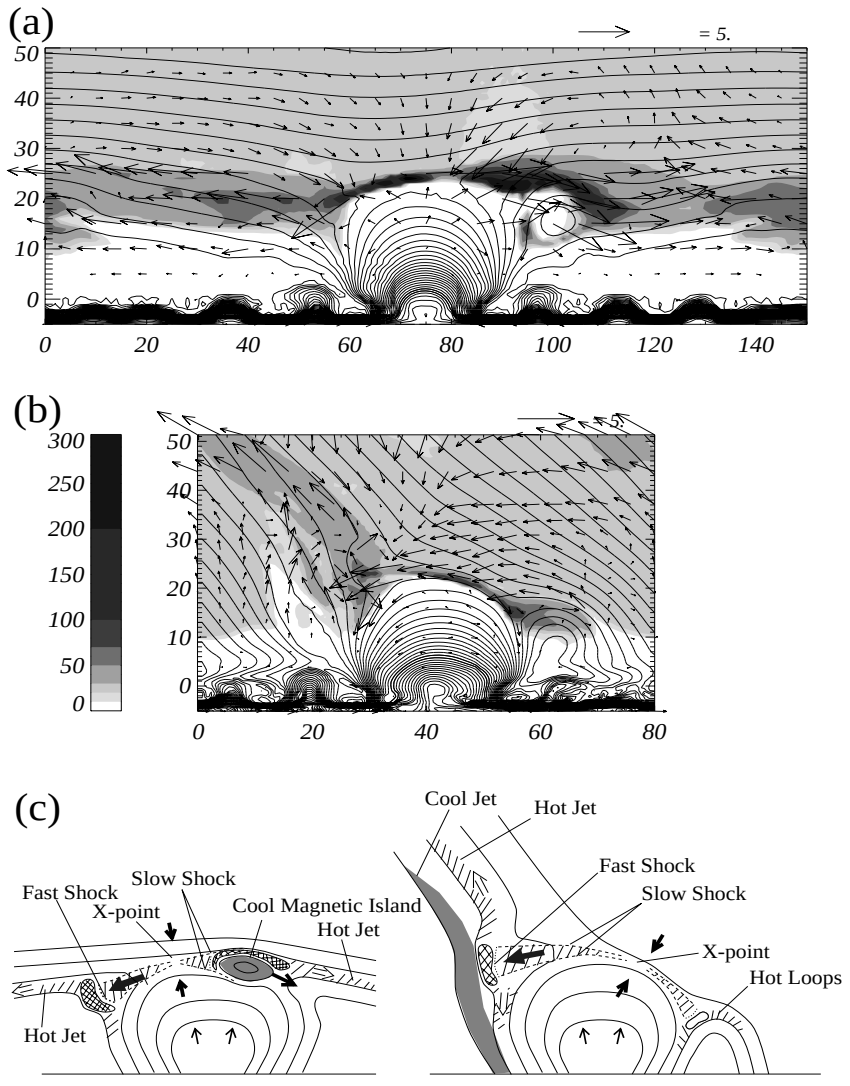

Figure 19: Schematic illustration of the physical processes found from numerical simulations of magnetic reconnection associated with emerging flux [218].

(2) *Fast Shock and Reconnection Point*: The reconnection jets from the X-point soon collide with the ambient field and form fast shocks (Fig. 19). The global jets emanate from the high pressure region just behind the fast shock, and propagate along the reconnected field lines. This suggests that *observed X-ray jets are not the*

reconnection jet itself, but hot jets accelerated by the enhanced gas pressure behind the fast shock.

The emission measure is smallest at the X-point, since the volume of the X-point is very small [218]. Thus the X-point is not bright and hence is not easily detected. This may be the reason why we observe a gap between a jet and the brightest part of a flare. In relation to this, Innes et al. [67] reported interesting observations of bi-directional plasma jets using SOHO/SUMER. They interpreted these jets as corresponding to reconnection jets because the intensity between the two jets was largest and hence (they thought) the brightest region corresponded to the X-point. However, as discussed above, the X-point cannot be a bright region, and hence it is likely that Innes et al. [67] observed a different phenomenon, e.g., bi-directional jets ejected from the high pressure region just behind the fast shock (see Fig. 19).

(3) *Hot and Cool Jets*: Not only hot jets ($T > 10^6$ K) but also cool jets ($T \sim 10^4 - 10^5$ K)are accelerated by the J x B force in association with reconnection (Fig. 19). The cool jets may correspond to Hα surges associated with X-ray jets [154], [21], [131]. These cool jets begin to be accelerated just before the hot jets are formed, and are ejected originally as plasmoids (or a helically twisted flux rope in three dimensions) and form an elongated structure after the plasmoids collide with the ambient fields. The initial phase of the ejection of both the cool and hot jets is seen as a *whip-like motion.* In the main phase, the cool jets are situated just to the side of the hot jets with nearly the same orientation. These features are indeed observed in several Hα surges associated with X-ray jets [21].

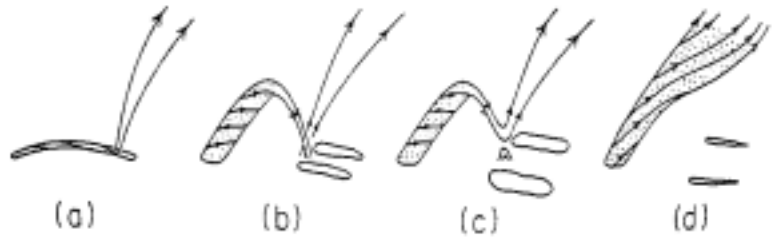

Figure 20: Schematic illustration of the formation of a spinning magnetic-twist jet as a result of reconnection between a twisted flux tube and an untwisted flux tube [151].

(4) *Spinning Jets and Alfven Waves*: Okubo et al. [131] and Yokoyama [221] extended Yokoyama and Shibata [217]'s simulations to the case in which twisted or sheared magnetic flux emerges and reconnects with the overlying field. They found that as a result of reconnection between the twisted (sheared) field and untwisted field, shear Alfven waves are generated and propagate along the reconnected field lines. Since these Alfven waves have a large amplitude, they excite a large transversal motion (or spinning motion) in the jets and exert a nonlinear magnetic pressure force on the cool/hot jets which causes them to be further accelerated, as originally suggested by Shibata and Uchida [151] (see Fig. 20). Canfield et al. [21] found that all Hα surges (9 events) in his observations showed spinning motion at a few 10 km/s, consistent with the prediction

from the numerical simulation. The direction of spin is also consistent with that of the unwinding motion of helically twisted flux tubes observed in the same active region 7260.

Kurokawa et al. [90] made beautiful observations of a spinning Hα jet using high spatial resolution velocity measurements at the Domeless Solar Telescope (DST) of Hida observatory. (See also Schmieder et al. [148] for observations of the spinning motion of Hα surges.) Pike and Mason [137] reported the discovery of a "solar tornado", rotating macrospicule like features, with SOHO/CDS. The rotating jet is also found from the morphological evolution of EUV jets observed with TRACE [5]. [6]

5 UNIFIED VIEW AND UNIFIED MODEL

As we have seen above, Yohkoh SXT/HXT observations have revealed various pieces of evidence of magnetic reconnection, especially the common occurrence of X-ray mass ejections (plasmoids and/or jets), in LDE flares, impulsive flares, and microflares. These are summarized in Table II. [7]

On the basis of this unified view, Shibata ([159], [161], [162]) proposed a unified model, the *plasmoid-induced-reconnection model*, to explain not only LDE and impulsive flares but also microflares and X-ray jets (Fig. 21). That is, the equations derived in the previous section can be applied to all these flares.

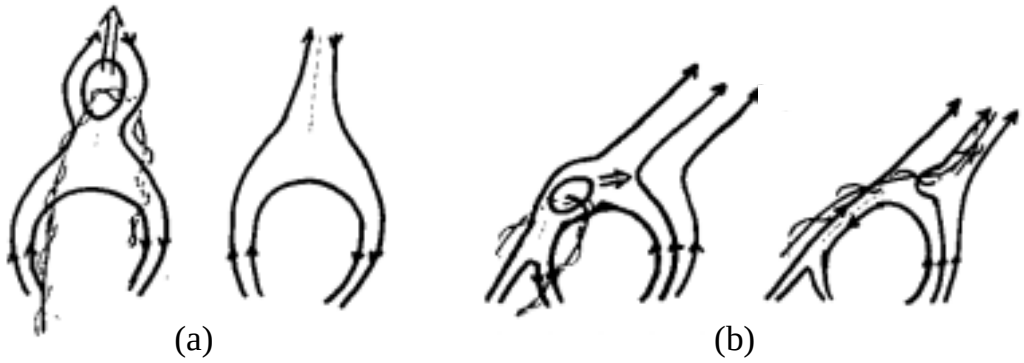

Figure 21: Unification of CSHKP model (a) and emerging flux model (b) by the *plasmoid-induced-reconnection* model [160], [161], [162]. Note that in (b), i.e., in the case of small scale flares, a plasmoid (a magnetic island or a helically twisted flux rope) collides and reconnects with the ambient magnetic field and disappears in a short time scale (10 – 100 sec).

One may argue, however, that the shape of X-ray jets and Hα surges (i.e., collimated jet-like structure) is very different from that of plasmoids. How can we relate these jets to plasmoids, the shapes of which are blob-like (or loop-like in three dimensional space) ? The answer to this question is already given by the numerical simulations of Yokoyama and Shibata ([217], [218]; Figs. 18 and 19); a blob-like plasmoid ejected from the current sheet soon collides with the ambient fields, and finally disappears (Fig. 18). The mass contained in

[6] See also related numerical simulations by Karpen et al. [71] on the reconnection between sheared and unsheared fields and the resulting formation of cool jets. On the other hand, Priest et al. [142] proposed the converging flux model as a model of X-ray bright points.

[7] See also the interesting unified view of solar flares and CMEs by Kahler et al. [73].

the plasmoid is transferred into the reconnected open flux tube and forms a collimated jet along the tube. In three dimensional space, this process would be observed as follows (see Fig. 21b): an erupting helical loop (a plasmoid ejected from the current sheet) collides with an ambient loop and induces reconnection, which is seen as a loop-loop interaction. Through this reconnection, magnetic twist (helicity) in the erupting loop is injected into the untwisted loop, resulting in the unwinding motion of the erupting loop/jet [151], which may correspond to the spinning motion observed in some Hα surges [21], [148]. This also explains why we usually do not observe plasmoid-like (or loop-like) mass ejections in smaller flares (e.g., microflares). In smaller flares, the current sheet is short, so that a plasmoid quickly collides with an ambient field and reconnects with it, thus disappearing. Hence the lifetime of the plasmoid (or loop-like) ejection is very short, of the order of $t \sim L/V_{plasmoid} \sim 10-100$ sec. It would be interesting to test this scenario using high spatial and temporal resolution observations with Doppler shift measurements using SOHO/SUMER, CDS and Solar B/EIS.

Table II Comparison of Various "Flares"

"flare"	size (L) (10^4 km)	time scale (t) (sec)	energy (erg)	mass ejection
microflares (ARTBs)	$0.5-4$	$60-600$	$10^{26}-10^{29}$	jet/surge
impulsive flares	$1-10$	$60-3\times10^3$	$10^{29}-10^{32}$	X-ray/Hα filament eruption
LDE flares	$10-40$	$3\times10^3-10^5$	$10^{30}-10^{32}$	X-ray/Hα filament eruption
large scale arcade formation	$30-100$	$10^4-2\times10^5$	$10^{29}-10^{32}$	X-ray/Hα filament eruption

Table II Comparison of Various "Flares" (continued)

"flare"	B (G)	n_e (cm^{-3})	V_A (km/s)	$t_A = L/V_A$ (sec)	t/t_A
microflares	100	10^{10}	3000	5	$12-120$
impulsive flares	100	10^{10}	3000	10	$6-300$
LDE flares	30	2×10^9	2000	90	$30-10^3$
large scale arcade formation	10	3×10^8	1500	400	$25-500$

Table III Unified View of Various "Flares"

"flares"	mass ejections (cool)	mass ejections (hot)
giant arcades	Hα filament eruptions	CMEs
LDE flares	Hα filament eruptions	X-ray plasmoid ejections/CMEs
impulsive flares	Hα sprays	X-ray plasmoid ejections
transient brightenings (microflares)	Hα surges	X-ray jets
EUV microflares	surges/spicules	EUV jets
facular points (nanoflares ?)	spicules	(Alfven waves)

Finally, we note that essentially the same physical process (magnetic reconnection associated with plasmoid ejections) can occur even below the transition region (see Table III). If the reconnection occurs in the upper chromosphere, the temperature of the heated plasma is of the order of $10^5 - 10^6$ K since the pre-heated plasma temperature is low ($\sim 10^4$ K) and the local plasma $\beta (= p_{gas}/p_{mag})$ is not low (> 0.01); note that the temperature of the reconnection-heated plasma is $\sim T_0/\beta$. EUV explosive events/jets (e.g., [31], [67]) may correspond to these reconnection events. If the reconnection occurs in the photosphere as suggested by recent MDI results [150], we would observe photospheric bright points (nanoflares) as well as mass flows with a velocity of a few – 10 km/s. This impulsive mass flow as well as large amplitude Alfven waves generated by the reconnection could be a source of energy which produces spicules and coronal heating ([86], [187], [146]).

6 ASTROPHYSICAL PLASMAS

6.1 Stellar Flares and Coronae

It is well known that stellar flares and coronae are very similar to solar flares and corona (e.g., [46], [47], [43]). Not only the light curves of stellar flare emissions (from radio, H alpha, visible continuum, to X-rays) but also the quantitative nature of flares, such as time

scales, plasma temperature, density, and magnetic field strength are all similar, although the range of temperatures and total energies of stellar flares is much broader ($T \sim 10^7 - 10^8$ K, total energy $10^{29} - 10^{37}$ erg) than those of solar flares ($T \sim (1-3) \times 10^7$ K, total energy $\sim 10^{29} - 10^{32}$ erg). It is believed that stellar flares are produced by a magnetic reconnection mechanism similar to that of solar flares. However, why do some stellar flares show such very high temperatures and extremely large total energies ?

Recent observations of young stars with the X-ray satellites ASCA and ROSAT have revealed that young stars such as protostars and T-Tauri stars frequently produce supehot flares with temperatures of 10^8 K ([84], [193], [66], see Feigelson and Montmerle [35] for a review). The time variation of the X-ray intensity (Fig. 22) is also similar to that of solar flares, while the total energy released during these flares amounts to $10^{36} - 10^{37}$ erg, much larger than in solar flares. Can these protostellar flares be explained by the same magnetic reconnection mechanism as that of solar flares ?

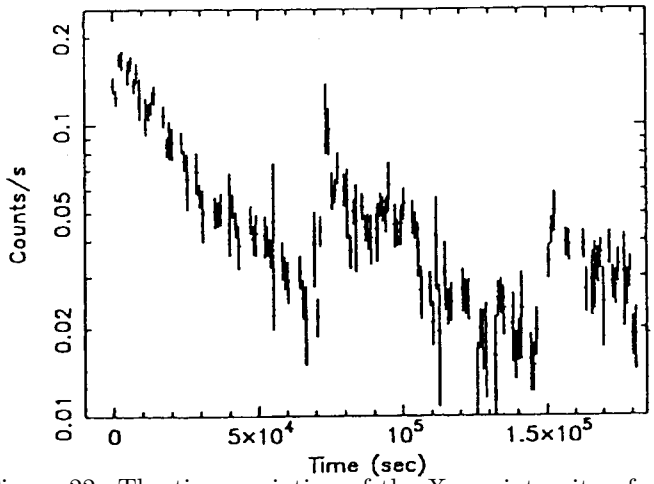

Figure 22: The time variation of the X-ray intensity of a protostellar flare on YLW15 observed with ASCA [200].

A hint is given by an interesting paper by Feldman et al. [36]. They showed that there is a universal correlation between the flare temperature (T) and emission measure (EM) not only for solar flares but also for some stellar flares. Shibata and Yokoyama [163] extended this universal correlation between T and EM to include solar microflares, T-Tauri star flares, and protostellar flares (Fig. 23). It is remarkable that the correlation holds over a very wide range, 4×10^6 K $< T < 10^8$ K and 10^{45} K $< EM < 10^{56}$ cm^{-3}. Shibata and Yokoyama [163] subsequently found that this universal correlation can be explained by a simple scaling law (see Fig. 23),

$$EM \simeq 10^{48}\ \mathrm{cm}^{-3} \left(\frac{B}{50\mathrm{G}}\right)^{-5} \left(\frac{n_0}{10^9 \mathrm{cm}^{-3}}\right)^{3/2} \left(\frac{T}{10^7 \mathrm{K}}\right)^{17/2}, \qquad (23)$$

which is derived from the following three equations:

$$EM = nL^3 \qquad (24)$$

$$2nkT = B^2/(8\pi) \qquad (25)$$

$$T = 10^7 \text{ K} \Big(\frac{B}{50\text{G}}\Big)^{6/7} \Big(\frac{n_0}{10^9 \text{cm}^{-3}}\Big)^{-1/7} \Big(\frac{L}{10^9 \text{K}}\Big)^{2/7}, \qquad (26)$$

where B is the magnetic field strength in the preflare corona, n_0 is the preflare coronal density, L is the flare loop length, and eq. (26) is based on the magnetic reconnection model with heat conduction and is the same as eq. (20).

Figure 23 shows that the universal correlation line corresponds to a constant magnetic field strength line for $30 - 150$ G, and indeed the coronal magnetic field strength is estimated to be about $40 - 300$ G for solar and stellar flares. In this figure, lines of constant loop length are also plotted, which show that the solar microflare loop length is $10^8 - 10^9$ cm, and the solar flare loop length is $10^9 - 10^{10}$ cm. These are fully consistent with observations. It is interesting to see that the stellar flare loop length is $10^{10} - 10^{12}$ cm, much larger than the loop lengths of solar flares. This is consistent with observations that the average field strength on the surface of young stars is very strong, of the order of kilo gauss, i.e., the filling factor of strong magnetic fields (i.e., star spots) is much larger than that on the Sun, indicating that the coronal loop size with strong magnetic fields (~ 100 G) is much larger than that on the Sun. The flare loop size in young stars is estimated to be comparable to or even larger than the solar radius ($\sim 7 \times 10^{10}$ cm). Consequently, we find that the reason why some stellar flares, especially young star flares, show very high temperatures and extremely large total energies is that the size of these flares is much larger than the size of solar flares. If the flare loop length is longer, even if the magnetic field is the same, the flare temperature increases in proportion to $L^{2/7}$ because the conduction cooling ($\kappa_0 T^{7/2}/L^2$) become less efficient for a longer loop. The total energy is simply determined by the total magnetic energy contained in the preflare coronal field, $\sim L^3 B^2/(8\pi)$, which explains the observations very well.

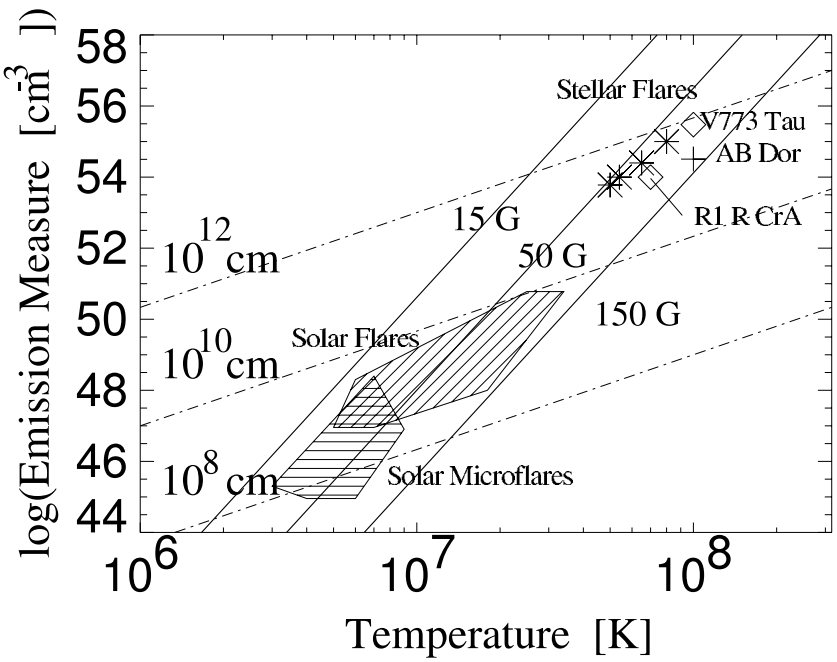

Figure 23: The universal correlation between emission measure and temperature for solar and stellar flares [163]. The solid lines show the theoretical scaling law $EM \propto B^{-5} T^{17/2}$ (eq. 23) for B = constant = $15, 50, 150$ G, and the dash-dotted lines show the EM-T relation for L = constant = $10^8, 10^{10}, 10^{12}$ cm.

Why is there such a large preflare coronal loop with a strong magnetic field ? Why is the filling factor for strong magnetic fields so large (near unity) in young stars ? One possibility is that the protostar is just born and keeps the primordial magnetic field, the origin of which is in the interstellar medium. The other possibility is that the strong magnetic field with a large filling factor is created by the dynamo action. Since the young stars rotate rapidly (> 30 km/s much faster than the solar rotation, ~ 2 km/s), the dynamo action would be stronger. It is also expected that there is an accretion disk (planet-forming disk) around the young star, so that strong magnetic interaction would occur between the central stellar core and the surrounding disk, which may lead to reconnection. Such a model has been developed by Hayashi, Shibata, Matsumoto [51], who performed 2.5D time dependent MHD numerical simulations of the interaction between an accretion disk and stellar magnetosphere (dipole magnetic field). They have shown that vigorous reconnection and associated mass ejections occur. Figure 24 shows a schematic illustration of their results.

This process is similar to that occurring in solar coronal mass ejections, and basic reconnection mechanism is the same as in solar flares (e.g., [195], [159], [220]). The reconnection releases huge amount of magnetic energy of order of 10^{36} erg (about 10^4 times more energetic than solar flares) stored in the sheared loop with a size of $L \sim 10^{11}$ cm.

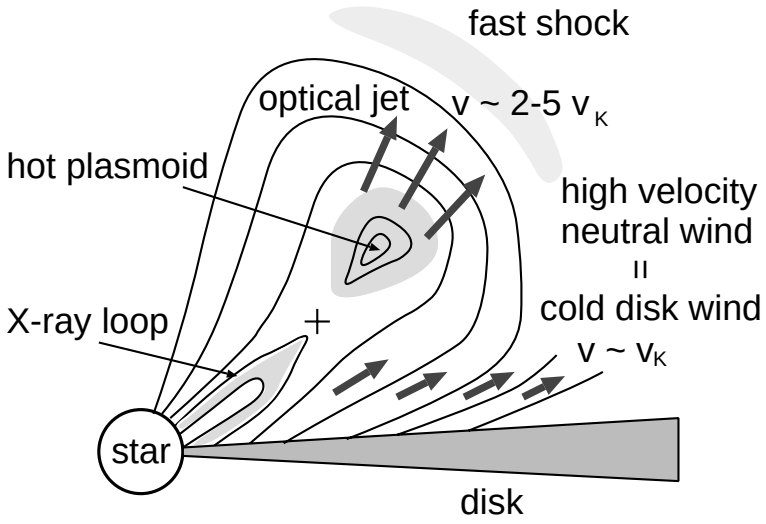

Figure 24: A schematic picture of the numerical results of Hayashi et al. [51]. The hot plasma jet ejected from the flaring region corresponds to the optical jet. The cold, dense wind emanating from the disk may explain high-velocity neutral winds.

6.2 Accretion Disks

Observations of accretion disks in X-ray binaries and active galactic nuclei show rapid time variations similar to those observed in solar flares in almost all of the electromagnetic spectrum (e.g., [123], [201]). Although there is no direct measurement of the magnetic field in these objects, the mechanism of the radio emission is known to be synchrotron radiation, so it is often assumed that equipartition magnetic fields are present in these objects. On the other hand,

recent progress in understanding accretion disk MHD (especially on the origin of viscosity; [12]) has revealed that the accretion disk is likely to have equipartition magnetic field strengths as a result of the nonlinear evolution of the magnetorotational instability ([52], [19], [110], [147]). Hence it is likely that the generated toroidal field would be buoyantly expelled out of the disk by the Parker (manetic buoyancy) instability (e.g., [109], [152]), thus forming a hot corona and flares around the disk by magnetic reconnection, similar to the case of the solar corona and flares [217]. Such an analogy between the solar corona and accretion disks (Fig. 25) has been proposed by Galeev et al. [42], and was developed recently by several researchers (e.g., [34], [97]).

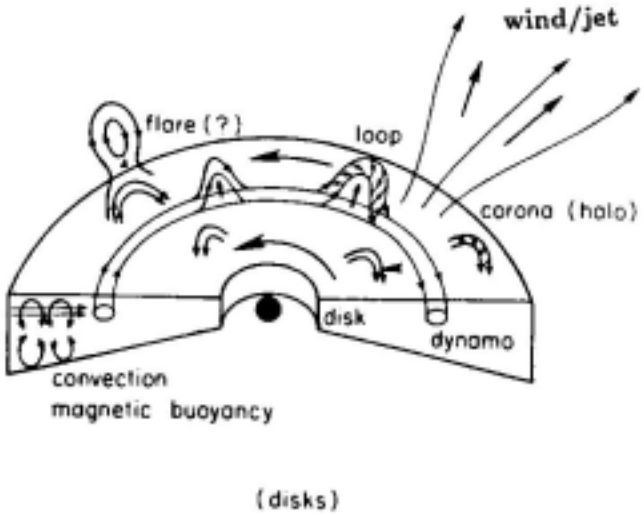

Figure 25: Schematic illustration of MHD processes in accretion disks [186].

Kawaguchi et al. [74] analyzed the results of 3D MHD simulations of accretion disks by Machida et al. [100], and showed that the rapid fluctuation of radiation from accretion disks, which shows a frequency dependence of $1/f^{\alpha}$ ($\alpha \simeq 1-2$) (e.g., [123]), can be reproduced by the time variability associated with magnetic reconnection and associated dynamical processes in accretion disks. They have also shown that the spatial structure of accretion disks becomes fractal with dimension $D = 1.9$. They argued that the self-organized criticality (SOC) ([11], [70]) is the key to understanding the basic mechanism which creates such time variability and fractal structure in accretion disks [119], as discussed in the solar flare context [99].

Finally, there is increasing evidence that the time variability of accretion disks may be related to the generation of jets, which reminds us of the relationship between solar flares and coronal mass ejections. Indeed, numerical simulations of jets ejected from magnetized accretion disks show that jets are often ejected in association with reconnection events similar to reconnection-ejection processes studied in protostellar flare models [51], (see Fig. 24). Reconnection might also play an important role inside the jet for the conversion of poynting energy to kinetic energy and for the acceleration of nonthermal particles (e.g., [18]). The same discussion may be applied

to gamma ray bursts (e.g., [176]).

6.3 Galaxies

In the disk of our Galaxy, the average magnetic field strength is measured to be a few μ G [13], and there are three components of the plasma, cold ($\sim$ 100 K), warm ($\sim 10^4$ K), and hot ($\sim 10^6$ K). The average plasma density is ~ 1 cm^{-3}, and hotter plasmas tend to have lower density, keeping the pressure roughly constant, although the fluctuation of the pressure is very large. It is also known that there is a hot plasma ($\sim 10^6$ K) in the halo of the Galaxy outside the disk (e.g., [136]), and there is even a superhot component ($1-10\times10^7$ K) in the disk called Galactic Ridge X-ray Emission (GRXE) [207], [83], [188]. GRXE is one of the most enigmatic phenomena in X-ray astronomy.

Note that the largest energy density in the Galaxy is the rotational energy $\sim 10^{-9}$ erg cm^{-3} which is much larger than the plasma internal energy $\sim 10^{-12}$ erg cm^{-3}, magnetic energy $\sim 10^{-12}$ erg cm^{-3}, and cosmic ray energy $\sim 10^{-12}$ erg cm^{-3}. The magnetic field can play the role of catalyst, converting rotational energy to plasma internal energy through dynamo action and reconnection. Such a role for magnetic reconnection has been discussed to explain hot plasmas in the galactic disk as well as in galactic halo [134], [103]. Sturrock and Stern [182] called the galactic reconnection "galactic flares".

Tanuma et al. [189], [190] performed the most extensive numerical simulations of reconnection triggered by a supernova shock in the context of galactic MHD, and applied the results to GRXE, i.e., superhot plasma ($\sim 10^8$ K) observed in the galactic disk. According to them, the hot component of GRXE can be explained if the magnetic field in the galactic disk is localized in an intense flux tube with $B \sim 30\mu G$ and a filling factor of < 0.1, similar to isolated flux tubes observed in the solar photosphere. Such a plasma with filamentary magnetic flux tubes is indeed found in the numerical simulations of magnetized accretion disks [100]. Tanuma et al. [190] also showed that magnetic reconnection starts long after a supernova shock passes a current sheet, and fast reconnection occurs once the current sheet becomes very thin through the occurrence of fractal-like tearing instability (see Fig. 26).

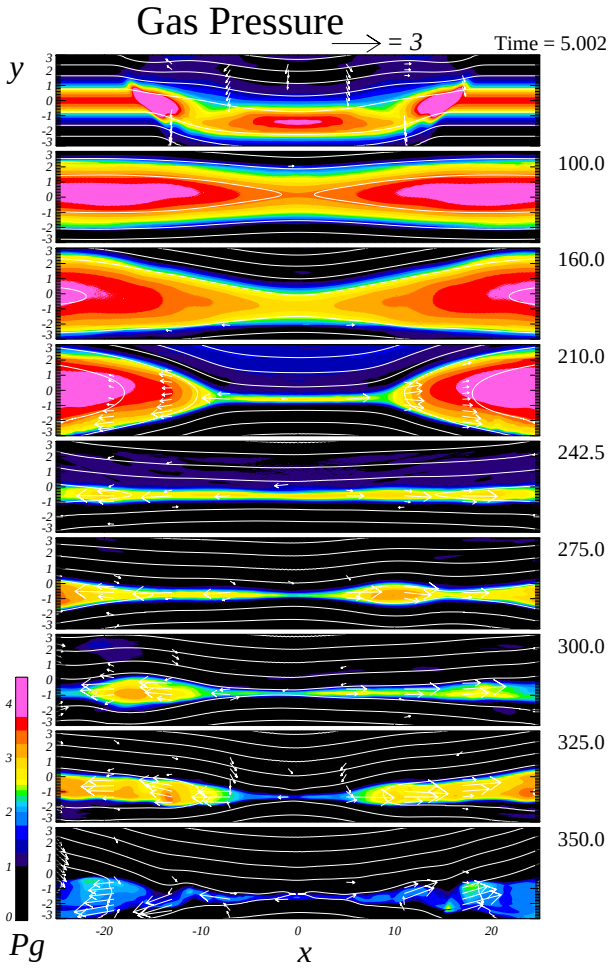

Figure 26: Numerical simulation of reconnection triggered by a supernova shock [190]. This illustrates a part of the scenario for fast reconnection (Fig. 13). Note that fast reconnection does not start just after the passage of the shock. Instead, the tearing instability is excited by the passage of the shock, and develops into Sweet Parker reconnection in its nonlinear stage. A secondary tearing instability occurs in the Sweet-Parker sheet, which then makes the current sheet thinner. Finally, the current sheet becomes thin enough to excite anomalous resistivity, leading to Petschek-like reconnection.

In clusters of galaxies, it is known that intergalactic space is filled with very hot plasmas with temperature $\sim 10^7 - 10^8$ K, density $\sim 10^{-4} - 10^{-2}$ cm^{-3}, and moderately strong magnetic fields with strength $1 - 40\mu$ G in the scale of $\sim 10^{24} - 10^{25}$ cm [23]. What is the origin of these hot plasmas ? In this case, the ultimate source of energy is gravitational energy, but the magnetic field may again play the role of catalyst. Makishima [103] discussed how hot plasma in clusters of galaxies may be heated by reconnection occurring between magnetically interacting galaxies, and Matsumoto et al. [111] modeled such an interaction using 3D MHD numerical simulations.

Magnetic reconnection in intergalactic plasmas and galaxy formation is now a frontier of plasma astrophysics [186].

7 REMAINING QUESTIONS AND PUZZLES

In spite of enormous progess in the understanding of magnetic reconnection in solar flares and the corona in the last 10 years, there still remain fundamental questions and puzzles:

(1) What determines the reconnection rate ? This is not a pure solar question, but a general plasma physics question. We should keep in mind that solar observations already show that fast reconnection occurs in both the case with and the case without apparent (macro-scale) driving forces during solar flares.

(2) Is solar reconnection of the Petschek type or Sweet-Parker type ? Or is it an other type ? Until now, we have not yet found clear evidence in favor of Petschek type reconnection, except that the reconnection rate is large, $0.001 - 0.1$.

(3) Where are the slow shock and fast shock associated with reconnection in solar flares. What is the true velocity of the reconnection inflow ?

(4) What is the energy buid-up process and the triggering mechanism of reconnection in solar flares ?

(5) What is the coronal heating mechanism ? Is it nanoflare heating (i.e., small scale reconnection heating) ? or Alfven wave heating ?

We expect that questions (2) - (5) will be clarified during Solar B mission era (2006 -), since Solar B carries very good telescopes and instruments which can observe velocity fields in the coronal reconnection region at a much better temporal and spatial resolution than Yohkoh and SOHO.

We should also keep in mind the very fundamental questions:

(6) How can we connect the macro-scale MHD and small-scale plasma processes ? Since the ratio of macro-scale (flare size) to small-scale (e.g., ion Larmor radius) is huge in solar flares as well as in astrophysical flares, we have a broad region whose length scale is much larger than the ion-Larmor radius (and thus MHD is applicable) but still much smaller than the observed scale in solar and astrophysical flares. What is actually occurring between the two extreme scales ?

(7) In relation to this, solar observations revealed that plasmoid ejections and time variability are ubiquitous not only in large scale flares but also in smaller scale flares. What is the role of plasmoid ejections and nonsteadiness in fast reconnection ?

(8) Observations of solar and cosmic flares universally show nonthermal emissions, and this is evidence of nonthermal particle acceleration. How are these nonthermal particles accelerated in association with magnetic reconnection ?

ACKNOWLEDGMENTS

The author would like to thank Prof. M. Ugai for his invitation to this book and also for his continual encouragement. He is also grateful to Dr. D. Brooks for his careful reading of the manuscript and many valuable comments, which were really useful for improving English of the manuscript, and to Mr. H. Tonooka and other Yohkoh colleagues for their various help and interesting discussions.

References

[1] Acshwanden, M. J., Hudson, H. S., Kosugi, T., and Schwartz, R. A., 1996, ApJ, 464, 985.

[2] Aschwanden, M., Poland, A. I., Rabin, D. M., 2001, ARAA, 39, 175.

[3] Acshwanden, M. J., & Parnell, C. E., 2002, ApJ, 572, 1048.

[4] Aschwanden, M., 2002, Space Sci. Rev., 101, 1.

[5] Alexander, D. M., and Fletcher, L., 1999, Solar Phys., 190, 167.

[6] Alfven, H., and Carlqvist, P. 1967, Solar Phys. 1, 220.

[7] Asai, A., Masuda, S., Yokoyama, T., et al., 2002, ApJ, 578, L91.

[8] Aurass, H., Klein, K. -L., and Martens, P. C. H., 1995, Solar Phys. Lett., 155, 203.

[9] Aurass, H., Vrsnak, B., Mann, G, 2002, A&A, 384, 273.

[10] Axford, W. I., McKenzie, J. F., Sukhorukova, G. V., Banaszkiewicz, M., Czechowski, A., Ratkiewicz, R., 1999, Space Sci. Rev., 87, 25.

[11] Bak, P., Tang, C., and Wiesenfeld, K., 1988, Phys. Rev., A, 38, 364.

[12] Balbus, S. A., and Hawley, J. F., 1991, ApJ, 376, 214.

[13] Beck, R., et al., 1996, ARAA, 34, 153.

[14] Benz, A. O., and Aschwanden, M. J., 1992, in Proc. Eruptive Solar Flares, IAU Colloq. No. 133, (eds.) Z. Svestka et al., Lecture Notes in Physics, 399, Springer-Verlag, Berlin, p. 106.

[15] Benz, A. O. and Krucker, S., 2002, ApJ, 568, 413.

[16] Biskamp, D., and Welter, H, 1989, Solar Phys., 129,49.

[17] Biskamp, D., 1997, Phys. Plasma, 4, 1964.

[18] Blandford, R. D., 2001, Prog. Theor. Phys. Suppl., 143, 182.

[19] Brandenburg, A. et al., 1995, ApJ, 446, 741.

[20] Burkepile, J.T., Cyr, O.C.St., 1993, A Revised and Expanded Catalogue of Mass Ejections Observed by the Solar Maximum Mission Coronagraph. HAO.

[21] Canfield, R. C., Reardon, K. P., Leka, K. D., Shibata, K., Yokoyama, T., and Shimojo, M., 1996, ApJ, 464, 1016.

[22] Cargill, P., and Priest, E. R., 1983, ApJ, 266, 383.

[23] Carrilli, C. L., and Taylor, G. B., 2002, ARAA, 40, 319.

[24] Carmichael, H., 1964, in Proc. of AAS-NASA Symp. on the Physics of Solar Flares, W. N. Hess (ed.), NASA-SP 50, p. 451.

[25] Cheng, C. Z. and Choe, G. S., 2001, Earth, Space, and Planets, 53, 597.

[26] Chen, P. F. and Shibata, K., 2000, ApJ, 545, 524.

[27] Choe, G. S., and Lee, L. C., 1996, ApJ, 472, 372.

[28] Choe, G. S., and Cheng, C. Z., 2000, ApJ, 541, 449.

[29] Cliver, E. W., 1983, Solar Phys., 84, 347.

[30] Dennis, B. R., 1985, Solar Phys., 100, 465.

[31] Dere, K., et al., 1991, JGR, 96, 9399.

[32] Dere, K., 1996, ApJ, 472, 864.

[33] Dere, K. et al., 1999, ApJ, 516, 465.

[34] di Matteo, T., 1998, MNRAS, 299, L15.

[35] Feigelson, E. D. and Montmerle, T., 1999, ARAA, 37, 363.

[36] Feldman, U., Laming, J. M., and Doschek, G. A., 1995, ApJ, 451, L79.

[37] Finn, J. M., and Kaw, P. K., 1977, Phys. Fluids, 20, 72.

[38] Forbes, T. G. and Priest, E. R. 1984, Solar Phys., 94, 315.

[39] Forbes, T. G., Malherbe, J. M., and Priest, E. R. 1989, Solar Phys., 120, 285.

[40] Forbes, T. G., 1990, JGR, 95, 11919.

[41] Forbes, T. G., Acton, L., 1996, ApJ, 459, 330.

[42] Galeev, A. A., Rosner, R., and Vaiana, G. S., 1979, ApJ, 229, 318.

[43] Güdel, M., 2002, ARAA, 40, 217.

[44] Gopalswamy, N., Payne, T. E. W. , Schmahl, E. J. , et al., 1994, ApJ, 437, 522.

[45] Gosling, J. T., 1993, JGR, 98, 18937.

[46] Haisch, B., Strong, K. T., and Rodono, M., 1989, ARAA, 29, 275.

[47] Haisch, B., and Schmitt, J. H. M. M., 1996, PASP, 108, 113.

[48] Hanaoka, Y., Kurokawa, H., and Saito, S., 1986, Solar Phys., 105, 133.

[49] Hanaoka, Y., et al., 1994, PASJ, 46, 205.

[50] Hanaoka, Y., 1996, Solar Phys., 165, 275.

[51] Hayashi, M. R., Shibata, K., and Matsumoto, R., 1996, ApJ, 468, L37.

[52] Hawley, J., Gammie, C. F., Balbus, S., 1995, ApJ, 440, 742.

[53] Heyvaerts, J., Priest, E. R. and Rust, D. M., 1977, ApJ, 216, 123.

[54] Hiei, E., Hundhausen, A. J., and Sime, D. G., 1993, GRL, 20, 2785.

[55] Hirayama, T., 1974, Sol. Phys., 34, 323.

[56] Hirayama, T., 1991, in Lecture Note in Physics, No. 387, Flare Physics in Solar Activity Maximum 22, ed. Y. Uchida et al. (New York, Springer), 197.

[57] Hirose, S., Uchida, Y., Uemura, S., et al., 2001, ApJ, 551, 586.

[58] Hori, K., Yokoyama, T., Kosugi, T., and Shibata, K., 1997, ApJ, 489, 426.

[59] Hoshino, M., Nishida, A., and Yamamoto, T., 1994, GRL, 21, 2935.

[60] Hu, Y. Q., 2001, Solar Phys., 200, 115.

[61] Hudson, H. S., 1994, in Proc. Kofu meeting, eds. S. Enome, and T. Hirayama, Nobeyama Radio Observatory , p. 1.

[62] Hudson, H. S. and Ryan, J., 1995, ARAA, 33, 239.

[63] Hudson, H. S., Acton, L. W., Harvey, K. L., and McKenzie, D. E., 1999, ApJ, 513, L83.

[64] Hudson, H. S., and Cliver, E. W., 2001, JGR, 10625.

[65] Hundhausen, A., 1998, in The many faces of the Sun: a summary of the results from NASA's Solar Maximum Mission, ed. K. T. Strong et al., Springer, New York, p. 143.

[66] Imanishi, K., Koyama, K., and Tsuboi, Y., 2001, ApJ, 557, 747.

[67] Innes, D. E., Inhester, B., Axford, W. I., et al., 1997, Nature, 386, 811.

[68] Isobe, H., Yokoyama, T., Shimojo, M., et al., 2002a, ApJ, 566, 528.

[69] Isobe, H., Shibata, K., Machida, S., 2002b, GRL, 29, 101.

[70] Jensen, H. J., 1998, Self-Organized Criticality, Cambridge Univ. Press, Cambridge.

[71] Karpen, J. T., Antiochos, S. K., DeVore, C. R., and Golub, L., 1998, ApJ, 495, 491.

[72] Kahler, S. W., Moore, R. L., Kane, S. R., and Zirin, H., 1988, ApJ 328, 824.

[73] Kahler, S. W., Reames, D. V., Sheeley, N. R. Jr., 2001, ApJ 562, 558.

[74] Kawaguchi, T., et al., 2000, PASJ, 52, L1.

[75] Khan, J. I., et al., 1998, A & A, 336, 753.

[76] Kitabata, H., Hayashi, T., Sato, T., et al. 1996, J. Phys. Soc. Japan, 65, 3208.

[77] Kliem, B., Karlicky, M., and Benz, A. O., 2000, A & A, 360, 715.

[78] Kopp, R. A., and Pneuman, G. W., 1976, Solar Phys., 50, 85.

[79] Kosugi, T., et al., 1991, Solar Phys. 136, 17.

[80] Kosugi, T., and Shibata, K., 1997, in Proc. Magnetic Storms, Geophysical Monograph 98, (Washington, American Geophysical Union), p. 21.

[81] Koutchmy, S., et al., 1997, A&A, 320, L33.

[82] Koutchmy, S., et al., 1998, in Observations of Plasma Astrophysics, Kluwer, p. 87.

[83] Koyama, K. et al., 1986, PASJ, 38, 121.

[84] Koyama, K., Ueno, S., Kobayashi, N., and Feigelson, E., 1996, PASJ, 48, L87.

[85] Krucker, S. and Benz, A. O., 1998, ApJ 501, L213

[86] Kudoh, T., and Shibata, K., 1999, ApJ, 514, 493.

[87] Kundu, M. R., Strong, K. T., Pick, M., et al., 1994, ApJ, 427, L59.

[88] Kundu, M. R., Raulin, J. P., Nitta, N., et al., 1995, ApJ, 447, L135.

[89] Kundu, M. R., Nindos, A., Raulin, J. -P., et al., 1999, ApJ, 520, 391.

[90] Kurokawa, H., Hanaoka, Y., Shibata, K. and Uchida, Y., 1987, Solar Phys., 108 , 251.

[91] Kusano, K., Suzuki, Y., and Nishikawa, K. 1995, ApJ, 441, 942.

[92] Lang, K. R., 2000, The Sun from Space, Springer.

[93] Lee, L. C., and Fu, Z. F., 1986, JGR, 91, 6807.

[94] Lin, J., and Forbes, T. G., 2000, JGR, 105, 2375.

[95] Lin, H. -A., Lin, R. P., and Kane, S. R., 1985, Solar Phys. 99, 263.

[96] Lin, R. P., et al., 1984, ApJ, 283, 421.

[97] Liu, B. F., Mineshige, S., and Shibata, K., 2002, ApJ, 572, L173.

[98] Litvinenko, Y. E., 1996, ApJ, 462, 997.

[99] Lu, E. T., and Hamilton, R. J., 1991, ApJ, 380, L89.

[100] Machida, M., Hayashi, M. R., and Matsumoto, R., 2000, ApJ, 532, L67.

[101] Magara, T., Shibata, K., Yokoyama, T., 1997, ApJ, 487, 437.

[102] Magara, T., Shibata, K., 1999, ApJ, 514, 456.

[103] Makishima, K., 1997, Plasma Phys. Control. Fusion, 39, A15.

[104] Makishima, K., 2001, Earth, Planets and Space, 53, 677.

[105] Martens, P. C. H., and Kuin, N. P. M., 1989, Solar Phys., 122, 263.

[106] Masuda, S., 1994, Ph. D. Thesis, U. Tokyo.

[107] Masuda, S., Kosugi, T., Hara, H., Tsuneta, S., and Ogawara, Y., 1994, Nature, 371, 495.

[108] Masuda, S., Kosugi, T., Hara, H., et al., 1995, PASJ, 47, 677.

[109] Matsumoto, R., et al., 1988, PASJ, 40, 171.

[110] Matsumoto, R., and Tajima, T., 1995, ApJ, 445, 767.

[111] Matsumoto, R., Valinia, A., Tajima, T., Makishima, K., and Shibata, K., 2000, Adv. Sp. Res., 25, 499.

[112] McCombie, W. J. and Rust, D. M., 1979, Solar Phys., 61, 69.

[113] McAllister, A. H., Kurokawa, H., Shibata, K., and Nitta, N., 1996a, Solar Phys., 169, 123.

[114] McAllister, A. H., et al., 1996b, JGR, 101, 13497.

[115] McKenzie, D. E., 2000, Solar Phys., 195, 381.

[116] McKenzie, D. E., and Hudson, H. S., 1999, ApJ, 519, L93.

[117] McKenzie, D. E., and Hudson, H. S., 2001, Earth, Planets, and Space, 53, 577.

[118] Mikic, Z., Barnes, D. C., and Scnack, D., 1988, ApJ, 328, 830.

[119] Mineshige, S., Takeuchi, M., and Nishihori, H., 1994, ApJ, 435, L125.

[120] Miller, J. A., Cargill, P. J., Emslie, A. G., et al., 1997, JGR, 102, 14631.

[121] Moore, R. L., and Roumeliotis, G. 1992, in Lecture Note in Physics, No. 399, Eruptive Flares, ed. Z. Svestka, B. V. Jackson, and M. E. Machado (New York, Springer), 69.

[122] Moore, R. L., Sterling, A. C., Hudson, H. S., and Lemen, J. R., 2001, ApJ, 552, 833.

[123] Negoro, H. et al., 1995, ApJ, 452, L49.

[124] Nitta, N., 1996, Proc. Bath Conf., Observations of Magnetic Reconnection in the Solar Atmosphere, Bentley, R. and Mariska, J. T. (eds.), ASP conf. ser., vol. 111, p. 156.

[125] Nitta, N., and Yaji, K., 1997, ApJ, 484, 927.

[126] Nitta, N., and Akiyama, S., 1999, ApJ, 525, L57.

[127] Nitta, S., Tanuma,S., Shibata, K., and Maezawa, K., 2001, ApJ, 550, 1119.

[128] Ohyama, M., and Shibata, K. 1997, PASJ, 49, 249.

[129] Ohyama, M., and Shibata, K. 1998, ApJ, 499, 934.

[130] Ohyama, M., Shibata, K., 2000, J. of Atmospheric and Solar-Terrestrial Physics, 62, 1509.

[131] Okubo, A. et al., 1996, Proc. Bath Conf., Observations of Magnetic Reconnection in the Solar Atmosphere, Bentley, R. and Mariska, J. T. (eds.), ASP conf. ser., vol. 111, p. 39.

[132] Ono, Y., et al., 2003, this volume.

[133] Parker, E. N., 1991, ApJ, 372, 719.

[134] Parker, E. N., 1992, ApJ, 401, 137.

[135] Parker, E. N., 1994, Spontaneous Current Sheets in Magnetic Fields, Oxford Univ. Press, New York.

[136] Pietz, J. et al., 1998, A&A, 332, 55.

[137] Pike, C. D. and Mason, H. E., 1998, Solar Phys., 182, 333.

[138] Porter, J. G., Fontenla, J. M., Simnett, G. M., 1995, ApJ, 438, 472.

[139] Priest, E. R., 2001, Earth, Planets, and Space, 53, 483.

[140] Priest, E. R., and Forbes, T. G., 2000, Magnetic Reconnection, Cambridge Univ. Press.

[141] Priest, E. R., and Forbes, T. G., 2001, A & A Rev. 10, 313.

[142] Priest, E. R., Parnell, C. E., and Martin, S. F., 1994, ApJ, 427, 459.

[143] Raulin, J. P., Kundu, M. R., Hudson, H. S. et al., 1996, A&A, 306, 299.

[144] Raymond, J. C., Cox, D. P., and Smith, B. W., 1976, ApJ, 204, 290.

[145] Sakai, J. I. and de Jager, C., 1996, Space Sci. Rev., 77, 1.

[146] Saito, T., Kudoh, T., Shibata, K., 2001, ApJ, 554, 1151

[147] Sano, T., and Inutsuka, S., 2001, ApJ, 561, 179

[148] Schmieder, B., K. Shibata, L. van Driel-Gesztelyi, and S. Freeland, 1995, Solar Phys., 156, 245.

[149] Scholer, M., 1989, JGR, 94, 8805.

[150] Schrijver, C. J., Title, A. M., van Ballegooijen, A. A., & Shine, R. A., 1997, ApJ, 487, 424

[151] Shibata, K., and Uchida, Y., 1986, Solar Phys., 103, 299.

[152] Shibata, K., et al., 1989, ApJ, 338, 471.

[153] Shibata, K., Nozawa, S., and Matsumoto, R., 1992a, PASJ, 44, 265.

[154] Shibata, K., Ishido, Y., Acton, L., et al., 1992b, PASJ, 44, L173.

[155] Shibata, K., Nitta, N., Strong, K. T., et al., 1994a, *in "X-ray Solar Physics from Yohkoh", eds. Y. Uchida et al., Univ. Academy Press*, p. 29.

[156] Shibata, K., Nitta, N., Strong, K. T., et al., 1994b, ApJ, 431, L51.

[157] Shibata, K., Masuda, S., Shimojo, M., et al., 1995, ApJ, 451, L83.

[158] Shibata, K., Yokoyama, T., and Shimojo, M., 1996, J. Geomag. Geoelectr., 48, 19.

[159] Shibata, K., 1996, Adv. Space Res., 17, (4/5)9.

[160] Shibata, K., 1997, in Proc. 5-th SOHO workshop, (ESA SP-404) p. 103.

[161] Shibata, K., 1998, in Proc. Observational Plasma Astrophysics, Watanabe, T., Kosugi, T., and Sterling, A. C. (eds), Kluwer, p. 187.

[162] Shibata, K., 1999, Astrophys. Space Sci., 264, 129.

[163] Shibata, K. and Yokoyama, T., 1999, ApJ, 526, L49.

[164] Shibata, K. and Tanuma, S., 2001, Earth, Planets, Space, 53, 473.

[165] Shibata, K. and Yokoyama, T., 2002, ApJ, 577, 422.

[166] Shimizu, T., Tsuneta, S., Acton, L. W., Lemen, J. R., Uchida, Y., 1992, PASJ, 44, L147.

[167] Shimizu, T., et al., 1994, ApJ, 422, 906.

[168] Shimizu, T., 1995, PASJ, 47, 251.

[169] Shimizu, T. et al., 2002, ApJ, 574, 1074.

[170] Shimojo, M., Hashimoto, S., Shibata, K., et al., 1996, PASJ, 48, 123.

[171] Shimojo, M., Harvey, K. K., Shibata, K., 1998, Solar Phys., 178, 379.

[172] Shimojo, M., and Shibata, K., 2000, ApJ, 541, 1100.

[173] Shiota, D., et al., 2003, PASJ, 55, L35.

[174] Simnett, G. M., et al., 1997, Solar Phys., 175, 685.

[175] Spicer, D. 1977, Solar Phys., 53, 305.

[176] Spruit, H. C., Daigne, F., and Drenkhahn, G., 2001, A & A, 369, 694.

[177] Sterling, A.C., Shibata, K., and Mariska, J.T., 1993, ApJ, 407, 778.

[178] Strong, K. T., Harvey, K., Hirayama, T., et al., 1992, PASJ, 44, L161.

[179] Sturrock, P. A., 1966, Nature, 211, 695.

[180] Sturrock, P. A., 1992, in Proc. Eruptive Solar Flares, IAU Colloq. No. 133, (eds.) Z. Svestka et al., Lecture Notes in Physics, 399, Springer-Verlag, Berlin, p. 397.

[181] Sturrock, P. A., 1999, ApJ, 521, 451.

[182] Sturrock, P. A. and Stern, R., 1980, ApJ, 238, 98.

[183] Svestka, Z., 1976, Solar Flares, Reidel.

[184] Svestka, Z. and Cliver, E. W., 1992, in Eruptive Solar Flares, Proc. IAU Colloq. No. 133, ed. Svestka, Z., Jackson, B., Machado, M. E., Springer, New York, p. 1.

[185] Tajima, T., et al., 1987, ApJ, 321, 1031.

[186] Tajima, T., and Shibata, K., 1997, Plasma Astrophysics, Addison-Wesley.

[187] Takeuchi, A., & Shibata, K., 2001, ApJ 546, L73.

[188] Tanaka, Y., 2002, A & A, 382, 1052.

[189] Tanuma, S., Yokoyama, T., Kudoh, T., et al., 1999, PASJ, 51, 161.

[190] Tanuma, S., Yokoyama, T., Kudoh, T., et al., 2001, ApJ, 551, 312.

[191] Terasawa, T., Shibata, K., and Scholer, M., 2000, Adv. Space Res., 26, 573.

[192] Tonooka, H., Matsumoto, R., Miyaji, S., et al., 2000, Adv. Space Res., 26, 473.

[193] Tsuboi, Y., Koyama, K., Murakami, H., et al., 1998, ApJ, 503, 894.

[194] Tsuneta, S., et al., 1991, Solar Phys., 136, 37.

[195] Tsuneta, S., et al., 1992a, PASJ, 44, L63.

[196] Tsuneta, S., et al., 1992b, PASJ, 44, L211.

[197] Tsuneta, S., 1996, ApJ, 456, 840.

[198] Tsuneta, S., 1997, ApJ, 483, 507.

[199] Tsuneta, S., et al. 1997, ApJ, 478, 787.

[200] Tsuneta, S., and Naito, T., 1998, ApJ, 495, L67.

[201] Ueno, S., Mineshige, S., Negoro, H., et al., 1997, ApJ, 484, 920.

[202] Uchida,Y. and Shibata,K., 1988, Solar Phys., 116, 291.

[203] Ugai, M., 1982, Phys. Fluids, 25, 1027.

[204] Ugai, M., 1986, Phys. Fluids, 29, 3659.

[205] Ugai, M., 1987, GRL, 14, 103.

[206] Ugai, M., 1994, Phys. Plasma, 1, 2853.

[207] Warwick, R. S., et al., 1985, Nature, 317, 218.

[208] Watanabe, T., 1994, in Proc. Kofu meeting, eds. S. Enome, and T. Hirayama, Nobeyama Radio Observatory , p. 99.

[209] Wang, Y. -M., Sheeley, N. R. Jr., Socker, D. G. et al., 1998, ApJ, 508, 899.

[210] Wang, Y. -M. and Sheeley, N. R. Jr., 1999, ApJ, 510, L157.

[211] Wang, Y. -M., Sheeley, N. R. Jr., Howard, R. A., et al., 1999, GRL, 26, 1349.

[212] Wang, Y. -M. and Sheeley, N. R. Jr., 2002, ApJ, 575, 542.

[213] Webb, D. F. and Cliver, E. W., 1995, JGR, 100, 5853.

[214] Yamamoto, T. T. et al., 2002, ApJ, 579, L45.

[215] Yashiro, S., and Shibata, K., 2001, ApJ, 550, L113.

[216] Yokoyama, T., and Shibata, K., 1994, ApJ, 436, L197.

[217] Yokoyama, T., and Shibata, K., 1995, Nature, 375, 42.

[218] Yokoyama, T., and Shibata, K., 1996, PASJ, 48, 353.

[219] Yokoyama, T., and Shibata, K., 1997, ApJ, 474, L61.

[220] Yokoyama, T., and Shibata, K., 1998, ApJ, 494, L113.

[221] Yokoyama, T., 1998, in Proc. Solar Jets and Coronal Plumes, ESA SP-421, p. 215

[222] Yokoyama, T., and Shibata, K., 2001, ApJ, 549, 1160.

[223] Yokoyama, T., et al., 2001, ApJ, 546, L69.

[224] Zhang, J., Kundu, M., White, S. M., et al., 2001, ApJ, 559, 452.